QA: QA

Model
Administrative Change Notice

Complete only applicable items.

1. Document Number:	MDL-NBS-HS-000010	2. Revision:	03	3. ACN:	01
4. Title:	Site-Scale Saturated Zone Transport				
5. No. of Pages Attached	42				

6. Approvals:		
Preparer:	Sharad Kelkar (Print name and sign) Sharad Kelkar	1/11/2008 (Date)
Checker:	Al Eddebbarh (Print name and sign) for Al Eddebbarh	01/11/2008 (Date)
QCS/Lead Lab QA Reviewer:	Sounia Kassabian-Darnell (Print name and sign) Sounia K. Darnell	01/11/2008 (Date)
Independent Technical Reviewer:	Ming Zhu (Print name and sign)	1/11/08 (Date)
Responsible Manager:	Kathryn Knowles (Print name and sign)	1/11/08 (Date)

7. Affected Pages	8. Description of Change:
x	Table of Figures: Updated listing for Figure 7-9b to reflect change to figure caption on p. 7-26 (see below).
3-2	Table 3-1: Changed "O.S 5.8&5.7" to "O.S 5.8 & 5.7" in fourth row, fourth column.
4-7	Table 4-2, footnote n: Added the following at the end of the footnote: "*SZ Flow Model.zip*, file: *SZ06.dat*, line 192, the ratio 2.236/0.447."
4-12	Section 4.1.2.13, first sentence: Added period at the end. Section 4.1.2.14, last paragraph: Changed "production" to "product".
6-2	Section 6.1, previous to the last paragraph of the section: Deleted a sentence about colloids because this statement referred to the DTN: LA0301AA831352.001 [DIRS 162433], which was found to have an error in it; the BTC reported for a tritium column experiment was incorrect. The DTN is being superseded, the impact of the change is expected to be minimal on downstream usage. It was judged that removing the sentence that referred to this DTN did not have a significant impact on the discussion; hence it was removed.
6-29	Table 6.4-3. Changed row 3 (parameters SCALEX and SCALEY), column 5 (source/DTN): added the following after *SZ Flow Model.zip*: "file: *SZ06.dat*, line 192".
6-30	Section 6.5, first sentence: Added file path "folder basecase\500Point" after citation of output DTN: LA0703SK150304.001.
6-38 and 6-39	Broke up the sentence into smaller parts, and made changes to the sentences to make them grammatically correct.
6-40	Table 6-7.1, Item 4, column 5: Changed 106 to 10^6.
6-41	Table 6-7.1, item 9, column 4: Added "(fraction)".

Model
Administrative Change Notice

Complete only applicable items.

1. Document Number:	MDL-NBS-HS-000010	2. Revision:	03	3. ACN:	01
4. Title:	Site-Scale Saturated Zone Transport				

6-46	Section 6.4.1.4, first paragraph, last sentence: Replaced “extreme” with “intermediate and high”.
6-50	Section 6.7.1.7, third sentence: Changed “production” to “product”.
6-53	Section 6.7.1.9: Added “As stated in Sections 4.1.2.7, 4.1.2.8, Table 6.4-2, and Table 6.7-1, the relationship between the flowing interval porosity, flowing interval spacing, and flowing interval aperture is that any one parameter value can be estimated using the other two parameters. Hence, out of these three parameters, any two can be independent.”
6-54	First paragraph, first sentence: Replaced “aperture” with “porosity”. Second paragraph, first sentence: Added text to first sentence; changed callout from Figure 6.7-8 to Figure 6.7-9.
6-58	Section 6.7.1.13, second paragraph, second sentence: Changed “production” to “product”.
6-62	Paragraph just before Section 6.8.2, line 4: Added text about dilution; deleted line 6.
7-1	Second and third paragraphs: Fixed paragraph justification. Next-to-last paragraph: Replaced “longer” with “shorter”.
7-26	Replaced Figure 7-9b. The path lines were labeled, and were shifted slightly to the east to be consistent with the Figure 7-9a. The visual validation is not affected by the shift. Also, the figure caption was corrected to correspond to the different coloring of the new path lines, and now reads “Transport Pathways Deduced from Hydrochemistry Data (in black, enlarged from Figure 7-9a) Overlaying Flow Paths Calculated from the Site-Scale Saturated Zone Transport Model (in blue) for Tracer Particles Starting at the Repository Footprint”.
9-15	Deleted reference entry for DIRS 162433.
A-7	Table A-2a: Modified footnote d to better explain the value in the table. Table A-2b: Added explanation to footnote b. This change addresses CR-10668.
A-31	First paragraph, first sentence: Changed “devitrified” to “zeolitic”.
B-1	Second paragraph, second sentence: Changed “Section 6.3.3.2” to “Section 6.3.12.2” in reference citation.
B-2	First paragraph, first sentence: Changed “Section 6.3.3.1” to “Section 6.3” in reference citation.
C-9	Tables C-2 and C-3: Added explanation to footnotes for output DTN: LA0309RP831321.001. This change addresses CR-10668.
C-11	Last paragraph, third sentence: Changed “Section C2.1” to “Section C1.1” in cross reference.
C-12	First paragraph, first sentence: Changed “Section C2.1” to “Section C1.1” in cross reference.
G-3	Table G-2, row for Mn^{2+}, column 4: Changed 0.0001 to 0.001. This change addresses CR-10668.
G-4	Table G-2, rows for alkalinity to ionic strength: Deleted. This change addresses CR-10668.

Model
Administrative Change Notice

Complete only applicable items.

1. Document Number:	MDL-NBS-HS-000010	2. Revision:	03	3. ACN:	01
4. Title:	Site-Scale Saturated Zone Transport				

G-5	Table G-3, column for surface areas: Changed values to be consistent with the source DTN: LA0412MD831341.001[DIRS 180906]. These changes do not affect any of the analysis or conclusions from this appendix. This change addresses CR-10668. Table G-3, source line: Removed DIRS 180904. Table G-3, NOTE: Changed to read, "Surface area measurements were conducted using a NOVA 1200 High Speed Gas Sorption Analyzer." This change addresses CR-10668.
G-10	Figure G-5, source line: Removed DIRS 180904.
G-11	Table G-6: Added "Abundance (wt%)" to the header and moved particle sizes to footnote. This change addresses CR-10668.
G-16	Tables G-7 and G-8: Deleted rows for porosity and pH; added NOTE to Table G-8. This change addresses CR-10668.
G-20	Table G-9: Deleted rows for porosity and pH. This change addresses CR-10668.
I-2	Table I-1: Added footnote. This change addresses CR-10668.
I-4	Table I-3: Corrected value of SiO_2 in column 3 and added footnote; in the row marked "PH", corrected the spelling to "pH" and in the last column changed entry to "N/A". These changes address CR-10668.
J-3	Table J-2: Changed values of SiO_2 and CO_3^{2-}; added footnotes d and e. This change addresses CR-10668.
K-3	Table K-2: Changed value of "upper limit" from 15×10^{-10} to 5×10^{-10}; removed citation of DIRS 149557 from source line.
NOTE: The changes noted above do not impact the method used, direct input sources, and product outputs or results.	

FIGURES (Continued)

Page

Table 3-1. Computer Software and Routines (Continued)

Software Title/Version Number	Software Tracking Number	Code Usage	Computer: Type, Platform, and Location	References
PHREEQC V 2.3	10068-2.3-01	Calculates surface complexation reactions for radionuclides.	PC Windows 2000 Location: LANL	[DIRS 157837]
RELAP V2.0	10551-2.0-00	Generate BTCs	PC, Windows 2000/NT Location : LANL	[DIRS 159065]
FRACT_p V1.0	11009-1.0-00	Calculates data that correlate concentrations with time for transport in the fractured media.	PC, LINUX 2.4.18, Location: LANL	[DIRS 164509]
fehm2post V.1.0	11031-1.0-00	Software is a set of perl scripts used to automate the repetitive series of steps required to make multiple runs of FEHM and post-process the output data.	WINDOWS 2000, SUN O.S 5.8 & 5.7, Redhat Linux 2.4.18	[DIRS 165754]
fehm2post V.1.0	11031-1.0-01	Software is a set of perl scripts used to automate the repetitive series of steps required to make multiple runs of FEHM and post-process the output data.	SUN O.S 5.9	[DIRS 181225]
EarthVision 5.1	10174-5.1-00	This software was used for plotting and visualization of data	Silicon Graphics Octane workstation running IRIX 6.5	[DIRS 167994]

LANL = Los Alamos National Laboratory; OS = operating system; PC = personal computer.

3.2 EXEMPT SOFTWARE

Commercial, off-the-shelf software used in support of this model report is listed in Table 3-2. This software is exempt from the requirements of IM-PRO-003, *Software Management*.

Table 3-2. Exempt Software

Software Name and Version	Description	Computer and Platform Identification
Microsoft Excel 2000	Used for preparing spreadsheets of data and plotting graphs. No data analysis was done with this software. Only built-in standard functions in this software were used. No software routines or macros were used with this software to prepare this report. The output was visually checked for correctness.	PC, Microsoft Windows 2000/NT

Table 4-2. Input Parameters and Range of Values for the Site-Scale Saturated Zone Transport Model (Continued)

Parameter	Base-Case Value(s)	Uncertainty Range	Units	Variable Type	Source/DTN
Dispersivity, transverse, vertical	0.0005	0.000005 to 0.1	m	Stochastic	Section 4.1.2.18

[a] The boundary fluxes, recharge rates and permeabilities were multiplied by this factor to vary the specific discharge. (The value of specific discharge is not directly input to the transport model, it is implicit in the flow fields. It has a base-case value of 0.36 m/yr from the repository to a distance of 5 km, as shown in SNL 2007 [DIRS 177391], Section 6.5.2.4.)

[b] Median value, given as the 0.5 probability value in the source data tracking number (DTN).

[c] Median value, interpolated to the 0.5 probability from the data given in the source DTN, *Table 6-8_updated.doc*, entry for parameter HAVO.

[d] Range derived from the normal distribution given in SNL 2007 [DIRS 181650], Figure 6-17.

[e] Base case is taken to be the value for nonsorbing radionuclides.

[f] These do not apply to the site-scale SZ transport model base case because the base case considers only the nonsorbing radionuclides and hence also excludes colloid facilitated transport.

[g] Base-case colloid sorption parameters are set to 0, and retardation factors set to 1, to simulate the base case of nonsorbing radionuclides.

[h] Each hydrostratigraphic unit was assigned a fixed value within this range.

[I] Flowing interval porosity is referred to as the "Fracture porosity in volcanic units," parameter FPVO, in DTN: SN0310T0502103.009 [DIRS 168763], *Table 6-8_updated.doc*.

[j] As discussed in Section 4.1.2.5, this value differs from that given in the reference DTN, but this is a conservative choice that avoids potential numerical problems.

[k] The value given here is lower than the value of 800 given in the source/DTN. This is a conservative choice.

[l] Note that the numbers in the source/DTN are in units of mg/L, which are converted to the units of this table, g/mL by multiplying by 10^{-6}.

[m] The lower limit given here is somewhat higher than the one given in the source/DTN and the upper limit given here is somewhat higher than that given in the source/DTN. This is a conservative choice.

[n] Value given in DTN: SN0612T0510106.004 [DIRS 178956], *SZ Flow Model.zip*, file: *SZ06.dat*, line 192, the ratio 2.236/0.447.

4.1.2.1 Specific Discharge Multiplier

Field values of groundwater-specific discharge in the saturated zone have been estimated from the tracer testing at the Alluvial Testing Complex as shown in *Saturated Zone In-Situ Testing* (SNL 2007 [DIRS 177394], Section 6.5.5) to be in the range of 0.46 to 9.4 m per year. This information is combined with the recommendations presented in *Saturated Zone Flow and Transport Expert Elicitation Project* (CRWMS M&O 1998 [DIRS 100353], p. 3-43) using Bayesian updating to create a distribution of the specific discharge multiplier in the range of 0.112 to 8.933 (SNL 2007 [DIRS 181650], Table 6-7[a]). All the permeabilities in the base-case flow model are multiplied by this factor, and all the recharge values and boundary fluxes input to the model are also multiplied by this factor to preserve the calibration of the base-case SZ flow model, as discussed in *Saturated Zone Site-Scale Flow Model* (SNL 2007 [DIRS 177391], Section 6.6; Tables 6-8 and 6-4[a]). The effect of the range of uncertainty in this parameter on the output BTCs is presented in Section 6.7.1. The base-case multiplier for the site-scale SZ transport model is chosen to be 1, corresponding to the median value used in the base-case SZ site-scale flow model.

4.1.2.12 Retardation Factor in Volcanics for Irreversible Colloids

Saturated Zone Colloid Transport describes the development of colloid retardation factors for fractured tuff from field and experimental data (BSC 2004 [DIRS 170006], Section 6.4). More details of this analysis are presented in *Saturated Zone Flow and Transport Model Abstraction* (SNL 2007 [DIRS 181650], Section 6.5.2.11) leading to an uncertainty distribution with a range of 6 to 800 and a median value of 26 (DTN: LA0303HV831352.002 [DIRS 163558]). The effect of the range of uncertainty in this parameter on the output BTCs is presented in Section 6.7.11. Base-case value for the site-scale SZ transport model is set to 1 to simulate the transport of nonsorbing radionuclides.

4.1.2.13 Groundwater Concentrations of Colloids

The uncertainty distribution was developed in *Waste Form and In-Drift Colloids-Associated Radionuclide Concentrations: Abstraction and Summary* (SNL 2007 [DIRS 177423], Section 6.3, DTN: MO0701PAGROUND.000 [DIRS 179310]). A range of 10^{-9} to 2×10^{-4} g/mL with a median value of 10^{-7} g/mL is given. This parameter enters the site-scale SZ transport model indirectly through the coefficient for reversible sorption onto colloids shown in *Saturated Zone Flow and Transport Model Abstraction* (SNL 2007 [DIRS 181650], Section 6.5.2.12). The effect of the range of uncertainty in this parameter on the output BTCs is presented in Section 6.7.12. The value of this parameter in the base-case transport model is set to 0 to simulate the transport of nonsorbing radionuclides.

4.1.2.14 Sorption Coefficient onto Colloids

The uncertainty distributions for the coefficient of sorption of plutonium, americium, thorium, protactinium, and cesium onto colloids were developed in *Waste Form and In-Drift Colloids-Associated Radionuclide Concentrations: Abstraction and Summary* (SNL 2007 [DIRS 177423], Section 6.3) and DTNs: MO0701PAKDSUNP.000 [DIRS 180392] and MO0701PASORPTN.000 [DIRS 180391]). A range of 1 (uranium and cesium on iron oxide corrosion product colloids) to 10^{7} (americium on smectite colloids) mL/g was used with a median value of 5×10^{5} mL/g (DTNs: MO0701PASORPTN.000 [DIRS 180391], Table 1-3, and MO0701PAKDSUNP.000 [DIRS 180392], Table 1-2). This parameter enters the site-scale SZ transport model indirectly through the coefficient for reversible sorption onto colloids. The effect of the range of uncertainty in this parameter on the output BTCs is presented in Section 6.7.12. The value of this parameter in the base-case transport model is set to 0 to simulate the transport of nonsorbing radionuclides.

4.1.2.15 Fraction of Colloids Transported Unretarded

A discussion of the fraction of colloids transported with no retardation is in *Saturated Zone Colloid Transport* (BSC 2004 [DIRS 170006], Section 6.6). The range of uncertainty distribution of this fraction is taken to be 0.00034 to 0.0017 with a median value of 0.0005. This parameter is applied in the TSPA calculations after the BTCs are calculated from the site-scale SZ transport model; hence, the influence of the uncertainty in this parameter on the BTCs is not discussed in this report. The base-case value is set to 0 to simulate the transport of nonsorbing radionuclides.

attached reversibly to the colloids using modified transport parameters (Section 6.4.2.6.2). Breakthrough curves for the radionuclides attached irreversibly to the colloids are generated using retardation factors for colloids (Section 6.4.2.6.1). A small fraction of colloids travels with the groundwater unretarded and is handled using the BTCs for nonsorbing radionuclides without the process of matrix diffusion.

A variety of laboratory and field data supports the understanding of the transport processes of importance included in the transport model. The cross-hole tracer tests conducted at the C-wells complex support the use of a dual-porosity fracture flow and transport model of advection and dispersion coupled with a matrix-diffusion and matrix-sorption model (*Saturated Zone In-Situ Testing*, SNL 2007 [DIRS 177394], Sections 6.3.3 and 6.3.4). Additionally, several laboratory-scale colloid-facilitated plutonium transport experiments conducted in fractured volcanic rocks support the use of a colloid-facilitated transport model in the volcanics (Kersting and Reimus 2003 [DIRS 162421], Chapter 7; and DTNs: LA0301PR831361.003 [DIRS 162435] and LA0301PR831361.004 [DIRS 162436]). The model of transport in the alluvium with advection, dispersion, sorption, and colloid-facilitated transport is supported by the single-well tracer tests at the Nye County Alluvial Testing Complex (ATC) wells as presented in *Saturated Zone In-Situ Testing* (SNL 2007 [DIRS 177394], Section 6.5). Laboratory column transport experiments in Yucca Mountain alluvium have indicated that sorption should be included in the alluvium transport model *Saturated Zone In-Situ Testing* (SNL 2007 [DIRS 177394], Section 6.5.6). These models are supported also by information available from analogue studies at the Nevada Test Site (NTS) (see Sections 7.1.1 and 7.1.2.6). The overall site-scale transport model is validated by comparison against transit times and flow paths deduced from hydrochemistry data (Section 7.2).

The site-scale SZ transport model is used directly in *Saturated Zone Flow and Transport Model Abstraction* (SNL 2007 [DIRS 181650]) for generating a set of radionuclide BTCs at the accessible environment for use in the TSPA simulations of radionuclide release to the biosphere. The outputs from the transport model are transit times, flow paths, and BTCs at the boundary of the accessible environment at 18 km for various radionuclides of concern. The results for the base case are given in Section 6.5.

6.2 FEATURES, EVENTS, AND PROCESSES

As stipulated in *Technical Work Plan for: Saturated Zone Analysis and Model Report Integration* (BSC 2006 [DIRS 177375]), this report addresses the saturated zone FEPs pertaining to the site-scale SZ transport that are included for TSPA (Table 6.2-1). Saturated zone FEPs for TSPA are given in DTN: MO0706SPAFEPLA.001 ([DIRS 181613], file *FEPs_be.mdb*, Table 7.1-1). Table 6.2-1 provides a list of FEPs that are relevant to this model analysis in accordance with their assignment in the LA FEP list. Specific reference to the various sections within this document where issues related to each FEP are addressed is provided in the table.

Table 6.4-2. Base-Case Model Inputs (Continued)

Input Name (Name of the Variable in the FEHM Code)	Input Description and Intended Use	Base-Case Value	Units	Type of Uncertainty	Source/DTN
statement “sptr”	dispersion calculations in Equations 1 and 20.				
ATV in the control statement “sptr”	Dispersivity, transverse, vertical, needed for dispersion calculations in Equations 1 and 20.	0.0005	m	Epistemic	Section 4.1.2.18

Source: Output DTN: LA0702SK150304.001.

[a] Epistemic uncertainty is defined as uncertainty in the parameter space of a conceptual model for which some knowledge is obtainable as given in BSC 2002 [DIRS 158794], Section 4.1.1.

[b] Input listed in Table 4-2 for flowing-interval porosity was multiplied by flowing interval spacing to obtain flowing interval aperture.

Table 6.4-3. Additional Parameters Needed for Abstraction Analysis

Input Name (Variable Name and the Control Statement where it Appears in the FEHM Code)	Input Description	Base-Case Value(s)	Units	Type of Uncertainty	Source/DTN
Multiplying factor[a] for SKD in control statement “flow”	Specific discharge multiplication factor	1	-	Stochastic	SN0706INPUTSZF.000 [DIRS 182007], file *updated_SZ_inputs_table.doc*
SCALEX[c], SCALEY[c] in control statement “fper,” ratio	Permeability horizontal anisotropy (HAVO) [c]	5[c]	-	Stochastic	SN0612T0510106.004 [DIRS 178956], file: *SZ Flow Model.zip*: file: *SZ06.dat*, line 192
RD_FRAC in the control statement “sptr,” ratio	Colloid retardation factor in volcanics for irreversible colloids	1	-	Epistemic	Table 4-2
Groundwater concentration of colloids Not a direct parameter in FEHM.	Needed in Equations 45 and 46 for calculating the relative concentration of radionuclide on colloids, which is in turn needed for colloid- facilitated reversible transport	0	g/mL	Epistemic	Table 4-2
Sorption coefficient onto colloids Not a direct parameter in FEHM.	Needed in Equations 45 and 46 for calculating the relative concentration of radionuclide on colloids, which is, in turn, needed for colloid- facilitated reversible transport	0	mL/g	Epistemic	Table 4-2

Table 6.4-3. Additional Parameters Needed for Abstraction Analysis

Input Name (Variable Name and the Control Statement where it Appears in the FEHM Code)	Input Description	Base-Case Value(s)	Units	Type of Uncertainty	Source/DTN
Fraction of colloids transported unretarded . Not a direct parameter in FEHM.	In TSPA calculations, used for post processing the BTCs generated by the transport model.	0.0005[b]	-	Epistemic	BSC 2004 [DIRS 170006], Section 6.6
Colloid retardation factor in alluvium and volcanics for irreversible colloids . Not a direct parameter in FEHM.	Used for calculating colloid sorption coefficient using Equation 22, which is in turn input as the variable K_d in the control statement "sptr," ratio	1	-	Epistemic	Table 4-2

[a] Base-case permeabilities and recharge and boundary fluxes are multiplied by this factor to vary specific discharge without affecting the flow calibration.
[b] This value is different from the base-case value given in Table 4-2. This parameter does not enter the base-case transport model directly. It is used in TSPA calculations for postprocessing the BTCs output from this report.
[c] Geometric mean of the permeability is preserved, thus the relationships used for calculating SCALEX and SCALEY from HAVO are : SCALEX=1/sqrt(HAVO) and SCALEY=sqrt(HAVO).

Infiltration rates enter the transport model only indirectly through the velocity field that is provided by the flow model. *Saturated Zone Site Scale Flow Model* (SNL 2007 [DIRS 177391], Section 6.4.3.9) notes that the increase in the updated infiltration estimates forms only 13% of the infiltration budget, and only 1% of the flow through lateral boundaries. An increased infiltration flux in the vicinity of the repository area can be expected to lead to higher specific discharge values in the volcanics, resulting in shorter travel times for the portions of the flow paths that reside in volcanics formation, thus leading to somewhat shorter overall travel times.

6.5 BASE-CASE MODEL RESULTS

The base-case model results (output DTN: LA0703SK150304.001, folder basecase\500Point) are discussed in this section. The conceptual and mathematical model described in Sections 6.3 and 6.4 was implemented in the numerical code FEHM V 2.24-01, a finite-volume/finite-element heat- and mass-transfer code that simulates nonisothermal, multiphase, multicomponent flow and solute transport in porous media. The details of this code, its usage and verification example are given in *Validation Test Plan (VTP) for the FEHM Application Version 2.24-01* (DOE 2007 [DIRS 181096]). The calibrated base-case site-scale SZ flow model (DTN: SN0612T0510106.004 [DIRS 178956]), which is described in detail in *Site-Scale Saturated Zone Flow Model* (SNL 2007 [DIRS 177391], Section 6.5), was used as the starting input.

The purpose of this model report is to provide a site-scale SZ transport model to be used as the starting point for the SZ abstraction model presented in *Saturated Zone Flow and Transport Model Abstraction* (SNL 2007 [DIRS 181650], Section 6.3) for use in the TSPA calculations. For this purpose, a single base-case transport model is presented here along with its outputs. The propagations of uncertainties in the input parameters to the output BTCs are presented in

Table 6.6-1b. Key Components and Basis for Alternative Conceptual Models Implicitly Included in the Site-Scale Saturated Zone Transport Model (Continued)

Alternative Conceptual Model	Key Components	Basis
Locally varying sorption parameters	Sorption parameters are strong functions of local water chemistry, rock mineralogy, and solute concentrations. The properties have to be calculated locally at each node along the travel path	The approach taken in this model report is to use linear transport equations with transport parameters appearing in the equations being treated as "effective" stochastic variables appropriate for the model scale. Transport parameters such as the K_d coefficients depend on type and concentration of the species, rock mineralogy, and groundwater composition including pH and Eh. As discussed in appendix A3, the range of groundwater compositions expected to occur in the saturated zone is taken into account in developing the small scale uncertainty distributions for K_ds. Given the current level of data available, water pH data are being treated as spatially random along the transport path, and oxidizing conditions are taken as a conservative approach, as justified in Section 6.3. To evaluate the effect of variations in rock mineralogy and scale on the K_d distributions, calculations were performed to calculate upscaled K_d distributions for the radionuclides uranium, neptunium, cesium, and plutonium. It was observed that the effective K_d distributions calculated for a single 500-m × 500-m grid block were narrower than the input K_d distributions. As discussed in appendix C2, the subject matter expert added a bias towards lower values to the CDFs. During performance assessment modeling studies, calculations will be made through multiple runs, each with a distinct K_d value sampled from the above-mentioned effective K_d distribution. This approach is more approximate than assigning K_d values on a node basis, as the latter approach will lead to breakthrough behavior that can be described by an even narrower distribution than the effective K_d distributions.
Channeling in alluvium	In alluvium, high-permeability channels exist that can provide preferential pathways for flow and transport	The conceptual model presented in this model report uses the effective-continuum approach, using effective values averaged over the grid block sizes on the order of 250 m × 250 m × 50 m for the parameters of interest, such as porosity. The effective porosity for alluvium being used in the TSPA calculations is represented by a normal distribution with the expected value of 0.18 and a value of 0.027 at 3 standard deviations below the mean shown in *Saturated Zone Flow and Transport Model Abstraction* (SNL 2007 [DIRS 181650], Section 6.5.2.3). Thus, the TSPA calculations allow for the eventuality that all the flow is concentrated within a small fraction of the alluvium, corresponding to the low effective porosity of 0.027. The conceptual and numerical model presented in this model report is appropriate for these ranges of values.

6.7 MODEL UNCERTAINTIES

Model-form uncertainty is presented in *Guidelines for Developing and Documenting Alternative Conceptual Models, Model Abstractions, and Parameter Uncertainty in the Total System Performance Assessment for the License Application* (BSC 2002 [DIRS 158794], Section 4.1.1).

This type of uncertainty in regards to the transport model is unavoidable given the sparseness of observed data and the limited amount of information available to corroborate or refute alternative models. This form of uncertainty is explicitly addressed by discussing alternative conceptual models in Section 6.6. The discussion and screening of the alternative conceptual models is based on available understanding and data. As discussed in Section 6.6, several of the alternative conceptual models can be accommodated within the current mathematical model framework by modifying the uncertainty distributions of the effective parameters (such as effective sorption coefficients and effective porosities) used in the model. Although the model is meant to represent the saturated zone transport accurately, for the case of those alternative conceptual models that could not be included in the model, the transport model was selected such that it resulted in transit times faster than those expected for the alternative conceptual model.

There are uncertainties associated with scaling parameter values from the scale of measurements to the scale of interest. Much of the data used for deriving parameter values in this report are from laboratory or field experiments conducted on spatial and temporal scales much smaller than those in the site-scale SZ model. Most of the measurements are done on sample sizes less than 1 m, with the exception of the C-wells and ATC field tests, which were conducted on the scale of tens of meters. This scale is still several orders of magnitude smaller than the site scale. Because the objective here is to calculate cumulative BTCs at a boundary of the accessible environment, large grid spacing (250 m × 250 m) is used in the numerical model. This leads to significant averaging of properties in the model calculations, thereby reducing the sensitivity of the output results to the stochastic variations in the parameter values. This is well demonstrated by the analysis presented in Appendix C for upscaling the distribution of the K_d values from a 4-m to a 500-m scale. These calculations demonstrate that the resulting 500-m-scale K_d distribution is actually narrower, for example, as shown in Table C-11 for uranium, with a standard deviation of 0.61 mL/g (and a mean of 6.61 mL/g) than the two starting 4-m-scale K_d distributions, shown in Table C-4, with mean and standard deviations of 2.0 mL/g and 0.6 mL/g, respectively in devitrified tuff, and 12.0 mL/g and 3.6 mL/g in zeolitic tuff, respectively. However, geological formations are inherently inhomogeneous, and they incorporate fractures, faults, and other heterogeneities on a variety of scales. Spatial correlations over some length scales often exist. Thus, it is difficult to extrapolate the measurements on a small scale to the SZ site scale.

As presented in *Guidelines for Developing and Documenting Alternative Conceptual Models, Model Abstractions, and Parameter Uncertainty in the Total System Performance Assessment for the License Application* (BSC 2002 [DIRS 158794], Section 4.1.1), there is epistemic uncertainty in the parameter space of the base-case conceptual model. This form of uncertainty is explicitly described by using probability distributions for appropriate model parameters. Expected uncertainty ranges for the various transport parameters are discussed in Section 4.1.2 and summarized in Table 4-2. The development and discussion of the K_d parameters needed for modeling reactive transport and the K_c parameters needed for modeling colloid-facilitated transport are presented in Appendices A, B, and C. The probability distributions for all other model parameters are presented and discussed in *Saturated Zone Flow and Transport Model Abstraction* (SNL 2007 [DIRS 181650], Sections 6.5.2 and 6.5.2[a]). These uncertainties are propagated through the model to the output BTCs, presented in Section 6.7.1. Radionuclide transit times are most sensitive to groundwater-specific discharge. This is because increasing the specific discharge not only increases the advective velocity but also reduces the time available

for matrix diffusion to be effective. In assessing the sensitivity of breakthrough times to the specific discharge through the model, permeabilities of the various units are scaled along with the specific discharge to preserve the model calibration. Other parameters of importance to the breakthrough times are matrix diffusion, the sorption coefficient in the volcanics as well as the alluvium, the effective flowing interval porosity in the volcanics (as reflected in the flowing interval aperture and spacing), the effective porosity in the alluvium, and the sorption coefficients for reversible colloids and retardation factor for irreversible colloids in the volcanics and alluvium. The volcanic retardation factors are important since the distribution contains large values that result in significant retardation even though transport times in the volcanics are shorter than the transport times in the alluvium. The contaminants spend the majority of the time in the alluvium; therefore, any retardation in the alluvium results in large effects in the overall transport time. Although the time for 50% breakthrough shows only a moderate sensitivity to the value of longitudinal dispersivity (Figure 6.7-14), the leading and tailing edges of the BTC are significantly affected for dispersivity values near the upper limit. Thus, dispersivity could be an important parameter to consider in situations where the first and last arrival times for radionuclides play an important role. Quantification of the sensitivity of the model output BTCs for various radionuclides of concern to parameter uncertainties are further evaluated in *Saturated Zone Flow and Transport Model Abstraction* (SNL 2007 [DIRS 181650], Sections 6.6, 6.7, and 8).

6.7.1 Propagation of Uncertainty in the Input Parameter Values to the Output

Starting with the SZ site-scale base-case transport model, sensitivity of the output BTCs to each of the uncertain input parameters was investigated by considering the upper and lower levels of each parameter individually (Table 6.7-1). The results presented here are limited to demonstrating the response of the model output to the extreme values of the input parameters given below.

Table 6.7-1. Effect of Parameter Ranges on 50-Percent Breakthrough Times

	Parameter	Base-case Value(s)	Uncertainty Range (Units)	Output Range, Time (Years) for 50% Breakthrough
1	Specific discharge multiplication factor[a]	1	0.112 to 8.933	31 to 52,840
2	Permeability horizontal anisotropy (north-south/east-west)	5	0.05 to 20 (ratio)	1,314 to 2,100
3	Bulk density in alluvium	1,910	1,669 to 2,151 kg/m^3	9,528 to 11,581
4	Sorption coefficient in alluvium	0.0	0 to 10,000 (mL/g)	810 to $>10^6$
5	Effective porosity in the alluvium	0.18	0. 02 to 0.3 (fraction)	709 to 986
6	Colloid retardation factor in alluvium for irreversible colloids	1	8 to 5,188 [e] (ratio)	1,859 to 688,357
7	Adjusted sorption coefficient for reversible sorption onto colloids in alluvium[b]	0	0 to 10,000 (mL/g)	245 to 7,023

Table 6.7-1. Effect of Parameter Ranges on 50 Percent Breakthrough Times (Continued)

	Parameter	Base-case Value(s)	Uncertainty Range (Units)	Output Range, Time (Years) for 50% Breakthrough
8	Flowing interval aperture[c] (holding Flowing Interval Porosity fixed at the base-case value of 0.001)	0.025773 (m)	1.86×10^{-5} to 8.0[d] (m)	166 to 6,653
9	Flowing Interval Porosity (holding the Flowing Interval Aperture fixed at the base-case value of 0.025773 m)	10^{-3}	10^{-5} to 10^{-1} (fraction)	132 to 9,008
9	Effective diffusion coefficient in volcanics	5.0×10^{-11}	5.0×10^{-12} to 5.0×10^{-10} (m^2/s)	245 to 6,324
10	Matrix sorption coefficient in volcanics	0.0	0 to 10,000 (mL/g)	810 to $>10^6$
11	Colloid retardation factor in volcanics for irreversible colloids	1	6 to 794 (ratio)	4,600 to 28,519
12	Adjusted sorption coefficient for radionuclides with reversible sorption onto colloids in volcanics	0	0 to 10,000 (mL/g)	165 to $>10^6$
13	Dispersivity, longitudinal	10.0	0.10 to 2,000 (m)	671 to 5,900

[a] Base-case permeabilities and the recharge and boundary fluxes are multiplied by this factor to vary specific discharge without affecting the flow calibration.

[b] See Equations 45 and 46 in Section 6.4.2.6.

[c] Flowing interval aperture is the product of the flowing interval porosity and flowing interval spacing.

[d] This value is made to address the case when flowing interval spacing is very large.

[e] The value used here is slightly lower than that given in Table 4-2.

6.7.1.1 Specific Discharge Multiplier

The results from simulations that evaluate the effect of changes in the specific discharge are shown in Figure 6.7-1. In these simulations, the base-case flow model was modified to scale the input recharge fluxes by the same factor as the rock permeabilities to preserve the model calibration. The results show that output is very sensitive to the level of uncertainty in this parameter. For the case of upper limit of specific discharge multiplier where the base-case fluxes are multiplied by a factor of 8.933, time to 50% breakthrough is 31 years (with extremely fast fluid flow such as would be expected for the very unlikely case of a high-permeability channel going continuously over the distance of 18 km in a highly faulted region). The lower limit of specific discharge multiplier, a factor of 0.112, leads to a breakthrough time of 52,840 years. This indicates that information that helps reduce the uncertainty of this parameter will greatly improve the ability of the model to predict the results.

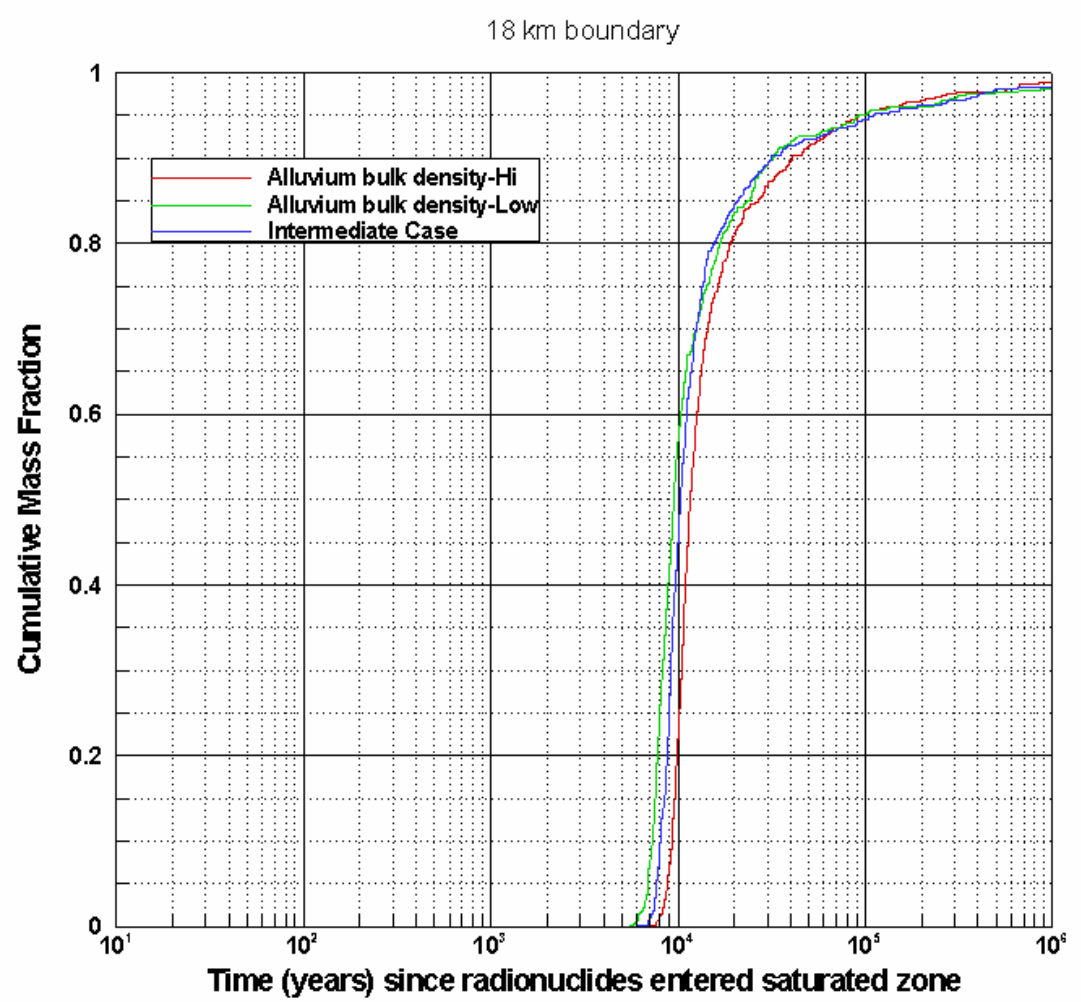

Output DTNs: LA0703SK150304.001, LA0703SK150304.003.

NOTE: Mass BTCs and median transport times are for an instantaneous source, present-day climate, and do not include radionuclide decay. Particle source location was near the middle of the anticipated repository footprint.

Figure 6.7-3. Propagation of Input Uncertainty in the Bulk Density of Alluvium to the Output Breakthrough Curves at the 18-km Boundary

6.7.1.4 Sorption Coefficient in Alluvium

The results from simulations that evaluate the effect of changes in sorption coefficient in alluvium on the output BTCs are shown in Figure 6.7-4. The results indicate that when the sorption coefficient is high (10,000 mL/g), no breakthrough of the tracers is observed in 10^6 years. Thus, the alluvium could form a very effective barrier for sorbing radionuclides. The base-case simulation is the same as for the low-sorption case because the base-case value of the sorption coefficient is 0, meant to represent the behavior of a nonsorbing radionuclide. For comparison, the green line in Figure 6.7-4 shows the breakthrough results for an intermediate value of the sorption coefficient of 6.3 mL/g, meant to represent a weakly sorbing radionuclide like neptunium. Since the base case does not have any retardation, transit times for both the intermediate and high cases are higher than that for the base case.

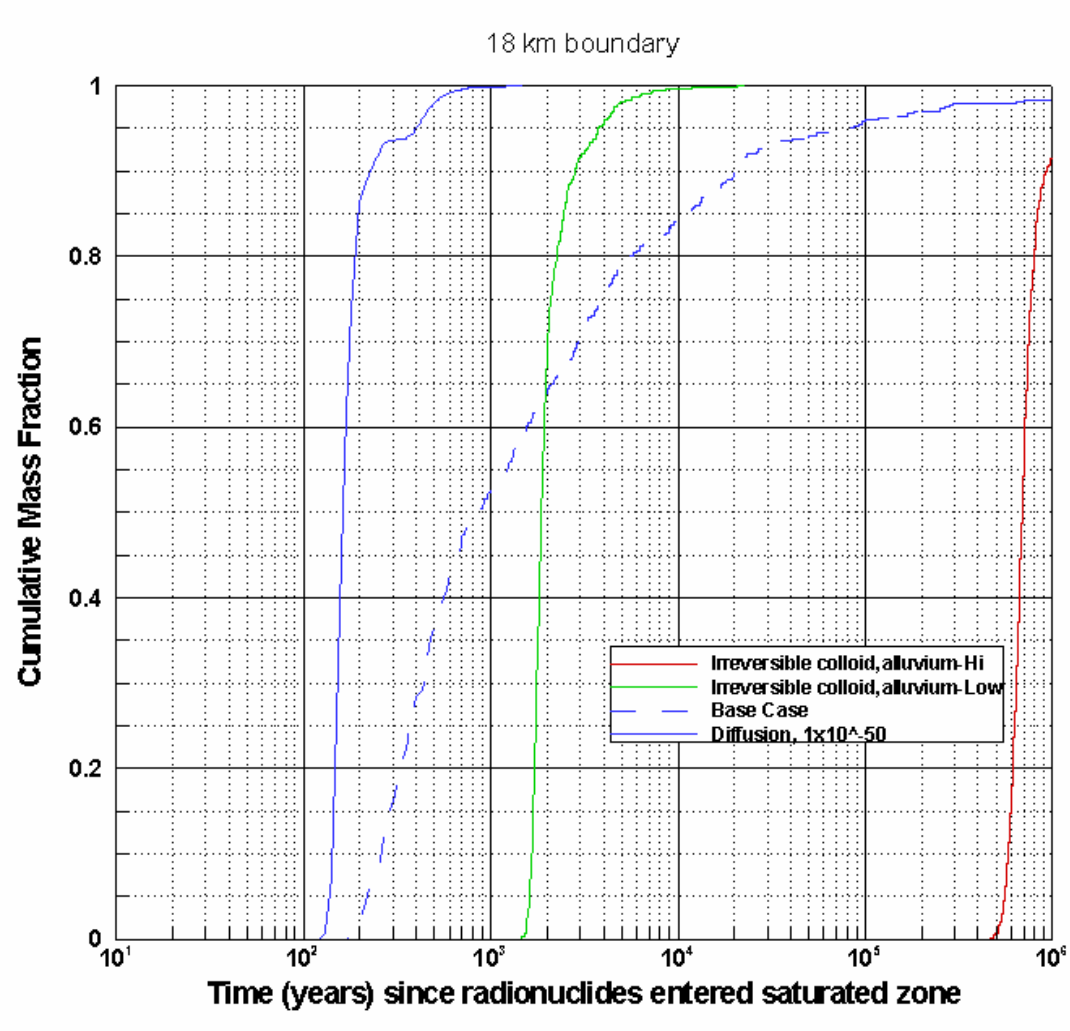

Output DTNs: LA0703SK150304.001, LA0703SK150304.004.

NOTE: Mass BTCs and median transport times are for an instantaneous source, present-day climate, and do not include radionuclide decay. Particle source location was near the middle of the anticipated repository footprint.

Figure 6.7-6. Propagation of Input Uncertainty in the Colloid Retardation Factor in Alluvium for Irreversible Colloids to the Breakthrough Curves at the 18-km Boundary

6.7.1.7 Reversible Sorption onto Colloids in the Alluvium

The results from simulations that evaluate the effect of changes in distribution parameters for reversible sorption onto colloids in alluvium are shown in Figure 6.7-7. The lower limit of the colloid concentration in groundwater (C_c) is 1.0×10^{-9} g/mL (Table 4-2). The minimum value for sorption onto colloids ($K_{d\text{-}c}$), 1.0 mL/g, occurs for uranium on iron oxide corrosion product colloids (Table 4-2), leading to the value of 10^{-9} for K_c. A minimum value of sorption coefficient (K_d) of 0.0 mL/g is used here as a conservative choice. The minimum value of the diffusion coefficient given in Table 4-2 is 5.0×10^{-12} m^2/s. For this case the minimum value of the adjusted effective diffusion coefficient ($D_e^{adjusted}$) in volcanics, computed using Equations 45a and 45b, is also 5.0×10^{-12} m^2/s, since K_c is much smaller than 1. This case is identical to the

For the case of high value of the aperture, the effect of diffusion is expected to be very small, as seen by comparing the red and the dashed-black curves in Figure 6.7-8. On the other hand, the case of low value of the aperture is expected to behave similar to a single porosity medium but with a larger value of the porosity, as seen from the fact that the green curve in the figure is delayed but approximately parallel to the red curve.

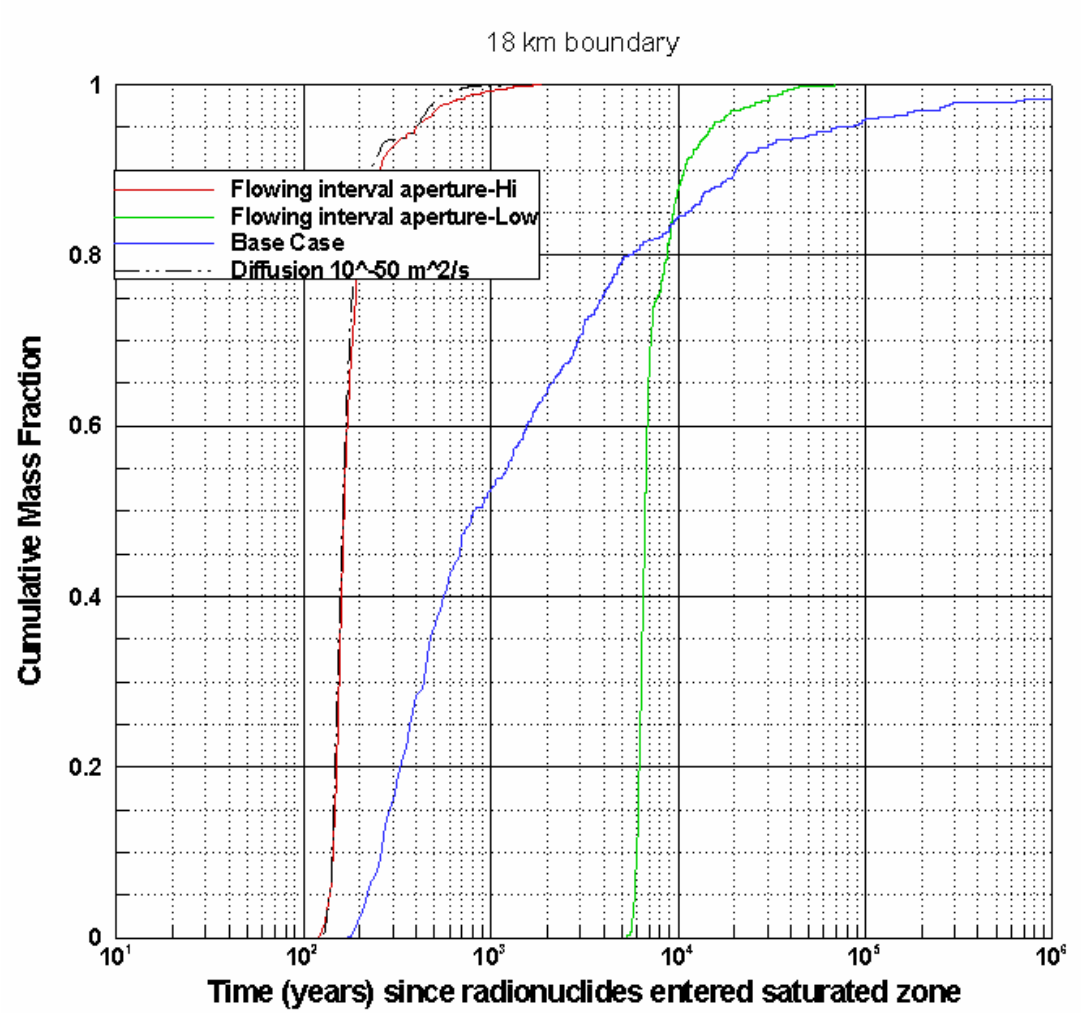

Output DTNs: LA0703SK150304.001, LA0703SK150304.005.

NOTE: Mass BTCs and median transport times are for an instantaneous source, present-day climate, and do not include radionuclide decay. Particle source location was near the middle of the anticipated repository footprint.

Figure 6.7-8. Propagation of Input Uncertainty in the Flowing Interval Aperture in Volcanics to the Breakthrough Curves at the 18-km Boundary

6.7.1.9 Flowing Interval Porosity in Volcanics

As stated in Sections 4.1.2.7, 4.1.2.8, Table 6.4-2, and Table 6.7-1, the relationship between the flowing interval porosity, flowing interval spacing, and flowing interval aperture is that any one parameter value can be estimated using the other two parameters. Hence, out of these three parameters, any two can be independent.

The results from simulations that evaluate the effect of changes in flowing interval porosity in volcanics (holding flowing interval aperture fixed at the base-case value of 25.773×10^{-5} m) on the BTCs are shown in Figure 6.7-9.

For the case of low value of the porosity, the flowing interval spacing is large, and hence the cross-sectional area available for diffusion is small, leading to a smaller effect of diffusion, as seen by comparing the green and the base case (blue) curves in Figure 6.7-9. On the other hand, the case of high value of the porosity is expected to behave similar to a single porosity medium but with a longer transit time, as seen from the fact that the red curve in the figure is delayed but approximately parallel to the green curve.

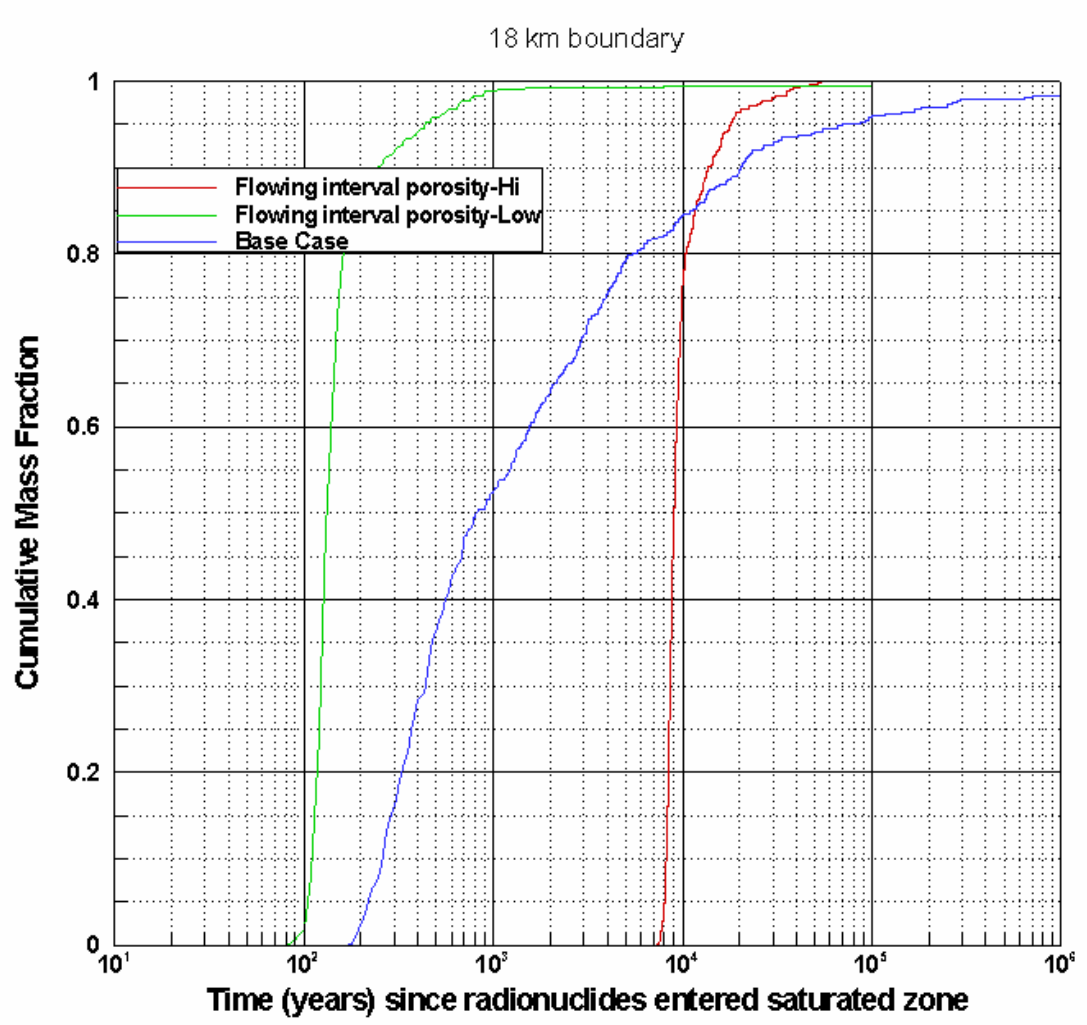

Output DTNs: LA0703SK150304.001, LA0703SK150304.005.

NOTE: Mass BTCs and median transport times are for an instantaneous source, present-day climate, and do not include radionuclide decay. Particle source location was near the middle of the anticipated repository footprint.

Figure 6.7-9. Propagation of Input Uncertainty in the Flowing Interval Porosity in Volcanics to the Breakthrough Curves at the 18-km Boundary

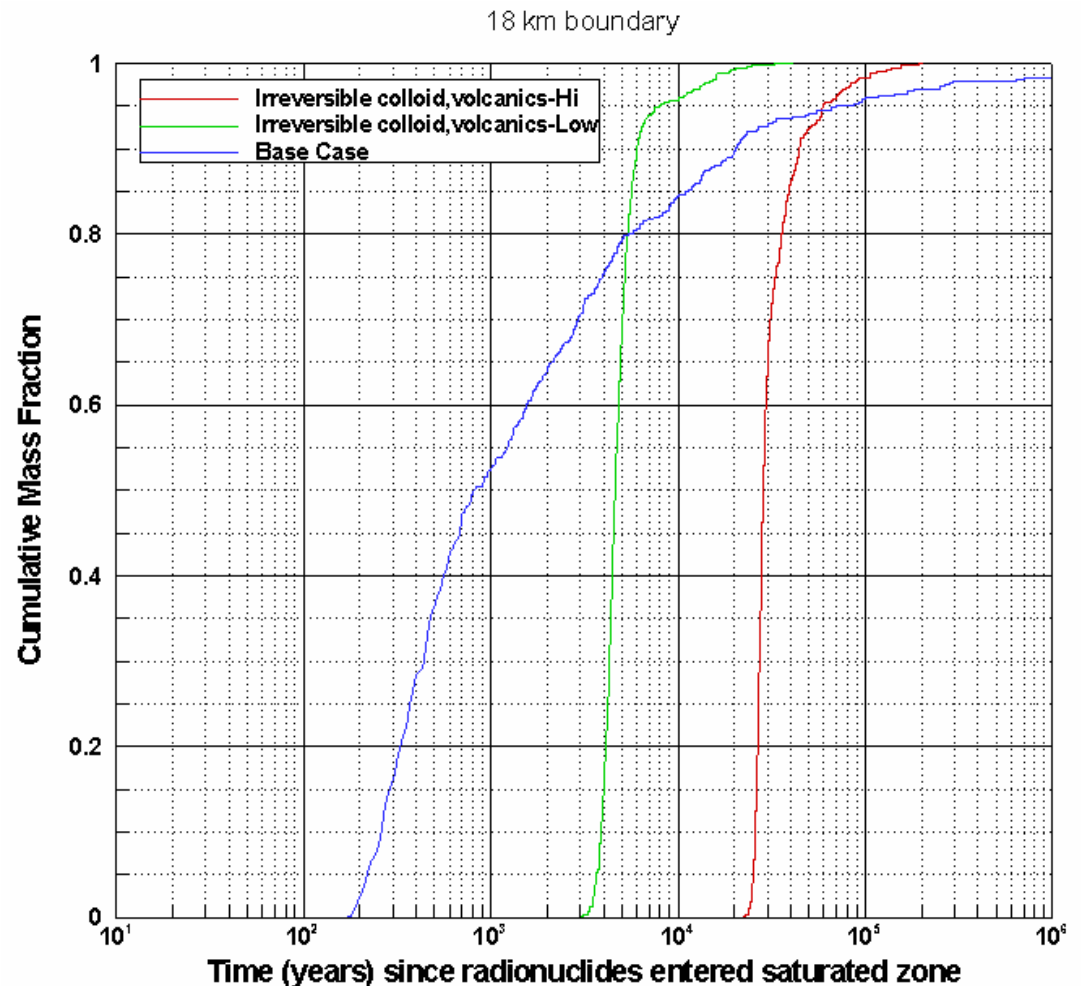

Output DTNs: LA0703SK150304.001, LA0703SK150304.004.

NOTE: Mass BTCs and median transport times are for an instantaneous source, present-day climate, and do not include radionuclide decay. Particle source location was near the middle of the anticipated repository footprint.

Figure 6.7-12. Propagation of Input Uncertainty in the Colloid Retardation Factor in Volcanics for Irreversible Colloids to the Output Breakthrough Curves at the 18-km Boundary

6.7.1.13 Reversible Sorption onto Colloids in the Volcanics

The process of colloid facilitated transport of radionuclides attached reversibly to colloids through volcanics is somewhat complicated, in that the effective diffusion ($D_e^{adjusted}$) is a function of the distribution parameter K_c, as given in Equations 45a, and 45b. The K_c in turn is a product of the concentration of colloids in the groundwater and the sorption coefficient for the radionuclide onto the colloids. The results from simulations that evaluate the effect of changes in the distribution parameter K_c for reversible sorption onto colloids in the volcanics are shown in Figure 6.7-13.

The lower limit of the colloid concentration in groundwater (C_c) is 1.0×10^{-9} g/mL (Table 4-2). The minimum value for sorption onto colloids ($K_{d\text{-}c}$), 1.0 mL/g, occurs for uranium on oxide corrosion product colloids (Table 4-2), and the minimum value of sorption coefficient onto

describes the technical basis for the saturated zone barrier in the context of the Yucca Mountain waste disposal system.

In its simplest form, the saturated zone performs two functions in its role as a barrier to radionuclide migration: (1) it delays the transport of radionuclides from beneath the repository to the boundary of the accessible environment at 18 km, and (2) it attenuates the concentration of radionuclides in the mobile water through the spreading and dilution of radionuclides that result from the processes of matrix diffusion, advection, and dispersion for various ranges of parameters. Also presented are intermediate BTCs at the contact between the fractured volcanic tuffs and the alluvium to assess the relative importance of the two key hydrostratigraphic rock types. Because all parameters are estimated rather than known with certainty, a few key parameters in this section are varied to complement the results from Section 8.3. Finally, transport simulations for the fraction of radionuclides bound to colloids are also examined because of the importance of this process to radionuclide transport predictions in the saturated zone.

6.8.2 Saturated Zone Subsystem Performance: Sorption in Volcanics and Alluvium

Most radionuclides are expected to sorb to the rock, which should delay their arrival at the boundary of the accessible environment at 18 km. Figure 6.8-1a also shows several simulations of sorbing radionuclides. The curve labeled "Matrix sorption" allows sorption in the matrix continuum of the volcanic tuffs and reflects a small matrix sorption coefficient of 1.3 mL/g. Including only this process yields a BTC similar to the base-case BTC but with significantly delayed transport times. The final curve in the figure shows the influence of sorption in the alluvium along with the fractured volcanics. Travel times largely in excess of 10,000 years are predicted in the saturated zone alone for a sorption coefficient of 6.3 mL/g, meant to fall in the range of K_d values for weakly sorbing radionuclides such as neptunium. It is seen from these curves that sorption in the alluvium can increase the transport time by orders of magnitude of even the weakly sorbing radionuclides such as neptunium (the results presented in Figure 6.8-1a do not include the effects of colloid-facilitated transport; those are discussed in Section 6.8.5).

6.8.3 Saturated-Zone Subsystem Performance: Fractured Volcanic Tuffs and Alluvium

To illustrate in more detail the function of the saturated zone, BTCs were computed at an intermediate location in the model at a boundary defined by the transition from fractured volcanic tuffs to alluvium. Figure 6.8-1b shows BTCs for the base-case and matrix sorption scenarios at the volcanic/alluvium boundary, which is approximately 11 km south of the southern boundary of the repository footprint. Comparing these simulations to the equivalent curves in Figure 6.8-1a, it is observed that the early parts of the BTCs differ from each other, but the latter parts are very close to each other. This shows that alluvium plays a significant role for short transport times. By contrast, the tails of the BTCs are due primarily to transport through fractures and matrix diffusion. Therefore, while the fractured volcanic tuffs provide significant delay for a fraction of the mass, the fastest moving portion of a radionuclide is controlled by transport through the alluvium. The reason for this result is that the continuum flow and transport through the bulk medium characterizes alluvium transport, in contrast to the fracture transport characterized by dual-porosity in the volcanics. Finally, based on the matrix sorption

7. VALIDATION

The site-scale SZ transport model is designed to provide an analysis tool that facilitates understanding of solute transport in the aquifer beneath and down gradient from the repository. It is also a computational tool for performing radionuclide migration predictions in the saturated zone. For these predictions to be creditable, it must be demonstrated that the site-scale SZ transport model has been validated for its intended use, which means there is established "confidence that a mathematical or numerical model and its underlying conceptual model adequately represents with sufficient accuracy the phenomenon, process, or system in question" (SCI-PRO-006, Attachment 1).

The validation activities for the site-scale SZ transport model are carried out according to *Technical Work Plan For: Saturated Zone Analysis and Model Report Integration* (BSC 2006 [DIRS 177375], Sections 2.1.4 and 2.2.4). The technical work plan (TWP) specifies level II validation. The BSC Level II validation is equivalent to Level I validation as described in SCI-PRO-002. Nevertheless, the site-scale SZ transport model was validated to Level II requirements. The Level II validation includes the six steps of confidence building during model development as described in SCI-PRO-002 and at least two post-development activities as described in SCI-PRO-006, Section 6.3.2. These validation activities do not generate a separate DTN.

To satisfy the model validation requirements, the following two postdevelopment validation activities (BSC 2006 [DIRS 177375], Section 2.2.4) were performed:

- Quantitative comparison of simulated transit times from beneath the repository to the accessible environment with those derived from isotopic data. Validation will be considered acceptable if the range of model results falls within the uncertainty estimates for groundwater ages from near the repository and from near the boundary of the accessible environment.

- Qualitative comparison of simulated flow paths with flow paths inferred from hydrochemistry and isotopic data. The model is considered valid if its flowpaths fall within those estimated by hydrochemical analyses.

This report deviates from *Technical Work Plan For: Saturated Zone Analysis and Model Report Integration* (BSC 2006 [DIRS 177375], Section 2.2.4.1) by excluding validation activity item #3. This item addresses the development of kinetics-based colloid transport model which was excluded from the scope of the work presented here. The purpose of the proposed kinetics-based colloid transport model was to reduce conservatism in the SZ transport model by using a more detailed model of the reversible filtration of the colloids with irreversibly attached radionuclides. Since the transport times predicted by the SZ transport model are shorter than those expected to result from the kinetic based model, this exclusion is considered acceptable.

As a result of the time and spatial scales involved and the fact that radionuclides cannot be used as tracers in field experiments, validation and confidence building for the site-scale SZ transport model relies on indirect data and inferences derived from technically related laboratory and field tests and natural analogues. Recognizing that the model is being used to perform probabilistic

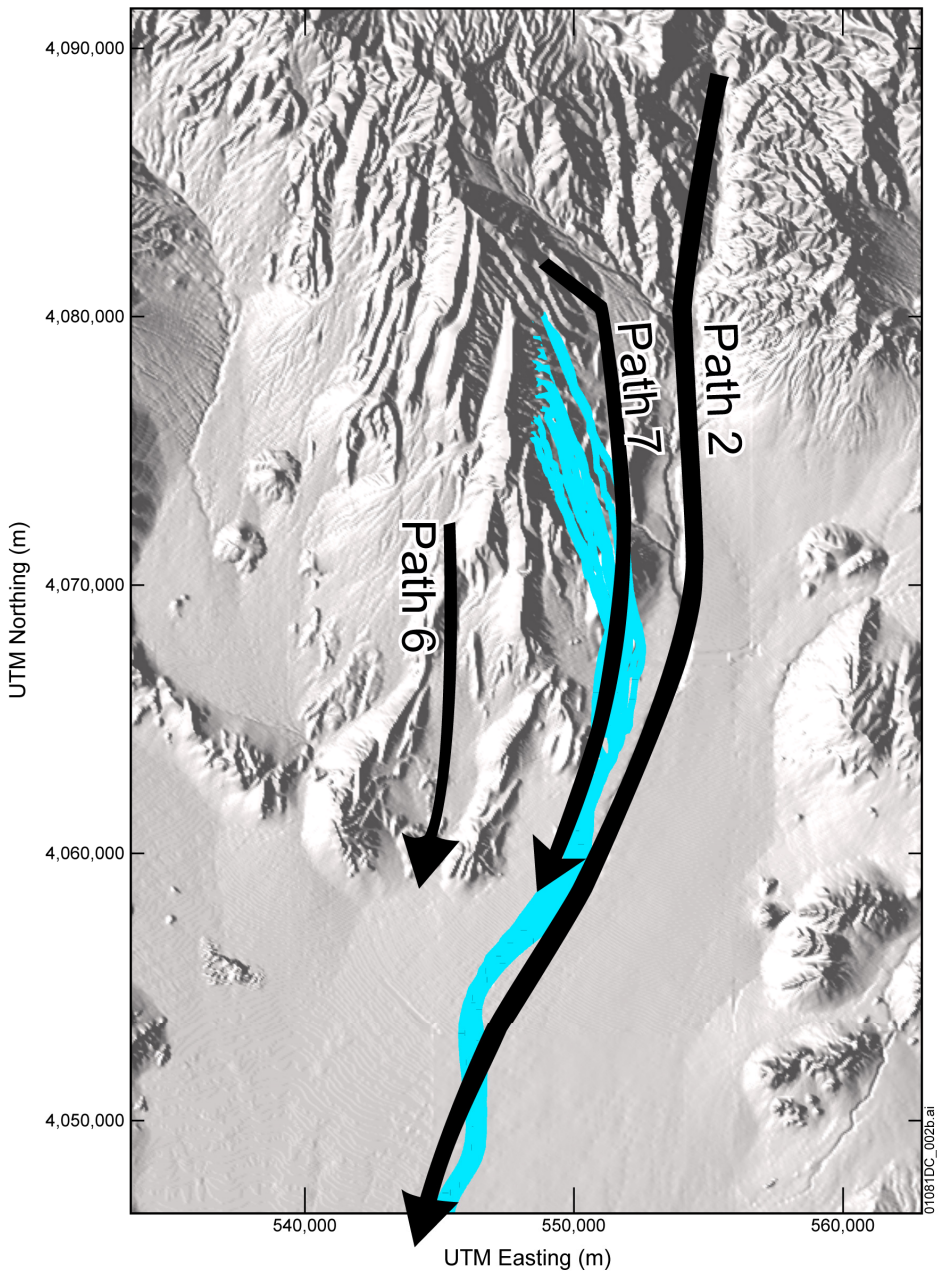

Source: Output DTN: LA0703SK150304.001.

Figure 7-9b. Transport Pathways Deduced from Hydrochemistry Data (in black, enlarged from Figure 7-9a) Overlaying Flow Paths Calculated from the Site-Scale Saturated Zone Transport Model (in blue) for Tracer Particles Starting at the Repository Footprint

148114 GS950808312322.001. Field, Chemical, and Isotopic Data Describing Water Samples Collected in Death Valley National Monument and at Various Boreholes in and Around Yucca Mountain, Nevada, Between 1992 and 1995. Submittal date: 08/16/1995.

145606 GS960308312133.001. Water Quality Data from Samples Collected in the Fortymile Wash Watershed, Yucca Mountain Area, Nevada, Water Year 1995. Submittal date: 03/27/1996.

182207 GS970700012847.002. Water-Quality Data from a Sample Collected at Well UE-25 C#3 on 5/18/95. Submittal date: 07/02/1997.

182209 GS970708312314.004. Water Chemistry Data from Three Samples Collected at Well UE-25 C#3, 12/4/96, 2/19/97, and 6/12/97. Submittal date: 07/16/1997.

149980 GS971000012847.004. Water Quality Data Collected from Springs and Wells in the Yucca Mountain Region from May 6, 1997 to May 15, 1997. Submittal date: 10/23/1997.

182212 GS980308312314.001. Water-Quality Data from a Suite of Samples Collected at UE-25 C #3 on 10/21/97. Submittal date: 03/26/1998.

145412 GS980908312322.008. Field, Chemical, and Isotopic Data from Precipitation Sample Collected Behind Service Station in Area 25 and Ground Water Samples Collected at Boreholes UE-25 C #2, UE-25 C #3, USW UZ-14, UE-25 WT #3, UE-25 WT #17, and USW WT-24, 10/06/97 to 07/01/98. Submittal date: 09/15/1998.

145611 GS990608312133.001. Ground-Water Quality Data. Submittal date: 06/09/1999.

107144 LA000000000086.002. Mineralogic Variation in Drill Core UE-25 UZ#16 Yucca Mountain, Nevada. Submittal date: 03/28/1995.

149557 LA0003JC831362.001. Preliminary Matrix Diffusion Coefficients for Yucca Mountain Tuffs. Submittal date: 4/10/2000.

156870 LA0109MD831341.001. Adsorption of NP-237 in Three Types of Alluvium as a Function of Time and Stratigraphic Position. Submittal date: 09/14/2001.

160051 LA0206AM831234.001. Eh-pH Field Measurements on Nye County EWDP Wells. Submittal date: 06/21/2002.

163852 LA0206AM831234.002. Geochemical Field Measurements on Nye County EWDP Wells. Submittal date: 06/21/2002.

p#1 (Table A-2a) and modified to have the sodium and bicarbonate compositions of this synthetic p#1 water (Table A-2b).

Table A-2a. Compositions of Waters from UE-25 J-13 and UE-25 p#1

Chemical Constituent	UE-25 J-13 Well Water[a] (mg/L)	UE-25 p#1 (Volcanics) Water[b] (mg/L)	UE-25 p#1 (Carbonate) Water[a] (mg/L)
Ca^{2+}	11.5	37	87.8
Mg^{2+}	1.76	10	31.9
Na^{+}	45	92	171
K^{+}	5 .3	5.6	13.4
SiO_2	64.2	49	37.3[d]
Cl^{-}	6.4	13	37
F^{-}	2.1	3.4[c]	3.5
SO_4^{2-}	18.1	38	129
HCO_3^{-}	143	344	698
pH	6.9	6.8	6.7

Sources: [a]Ogard and Kerrisk 1984 [DIRS 100783].
[b] DTN: MO0007MAJIONPH.011 [DIRS 151524].
[c] DTN: SN0705FLUORINE.001 [DIRS:182006].
[d] Value derived from Table III of Ogard and Kerrisk 1984 [DIRS 100783], equivalent to 0.62 mmol/L Si.

Table A-2b. Comparative Information on the Range of Concentrations from Wells in the Saturated Zone Transport Model Area

Chemical Constituent	Range of Concentrations in Downgradient Wells in Volcanics[a] (mg/L)	Range of Concentrations in Downgradient Wells in Alluvium[a] (mg/L)	Synthetic p#1 Water (mg/L)
Ca^{2+}	0.8 to 37	0.8 to 20.3	
Mg^{2+}	< 0.1 to 10	0.0 to 7.7	
Na^{+}	38 to 120	57.9 to 180.5	261[b]
K^{+}	1.1 to 8.9	1.8 to 5.5	
SiO_2	36 to 57	40.5 to 61	
Cl^{-}	6.0 to 13	5.6 to 18	
F^{-}	1.0 to 6.7	1.6 to 4.2	
SO_4^{2-}	14 to 38	18.7 to 61.7	
HCO_3^{-}	107 to 344	110 to 255.5	691[b]
CO_3^{2-}	0.0	0.0 to 23.5	
pH	6.8 to 8.4	7.5 to 8.9	
Eh	-	128 to 197 mv	-

Sources: [a] SNL 2007 [DIRS 177391], Table A6-1.
[b] Estimated from information provided by Triay et al. (1996 [DIRS 101024], p. 4), as follows: The synthetic UE-25p#1 water was prepared by dissolving 0.39 g of Na_2CO_3 and 8.90 g of $NaHCO_3$ in 10 liters of deionized water. Thus, the primary source of HCO_3^{-} is from dissolution of $NaHCO_3$ (890 mg/L) and additional contribution by added CO_3^{2-} (39 mg/L), which was estimated by treating it as being completely converted to HCO_3^{-}. This is a reasonable treatment for the pH range of interest of 6.8 to 8.4 (Langmuir 1997 [DIRS 100051], Figure 5.2, p. 156). The HCO_3^{-} from $NaHCO_3$ was (61/(23+61))*890 = 646.31 (mg/L), and that from Na_2CO_3 was (2*[(60/(23*2+60))*39] = 44.14 mg). 691 is an approximation of the sum of the two contributions.

A4. EXPERIMENTAL TECHNIQUES

The basic technique for the laboratory determination of sorption coefficients involved the contact of a groundwater sample, spiked with the radionuclide of interest, with a crushed sample of tuff or alluvium (Daniels et al. 1982 [DIRS 105803]). The rock sample was generally obtained as a core sample. The core was crushed in a jaw crusher and subsequently sieved to a selected grain-size fraction. The sieving process was usually carried out under water. Initially, several

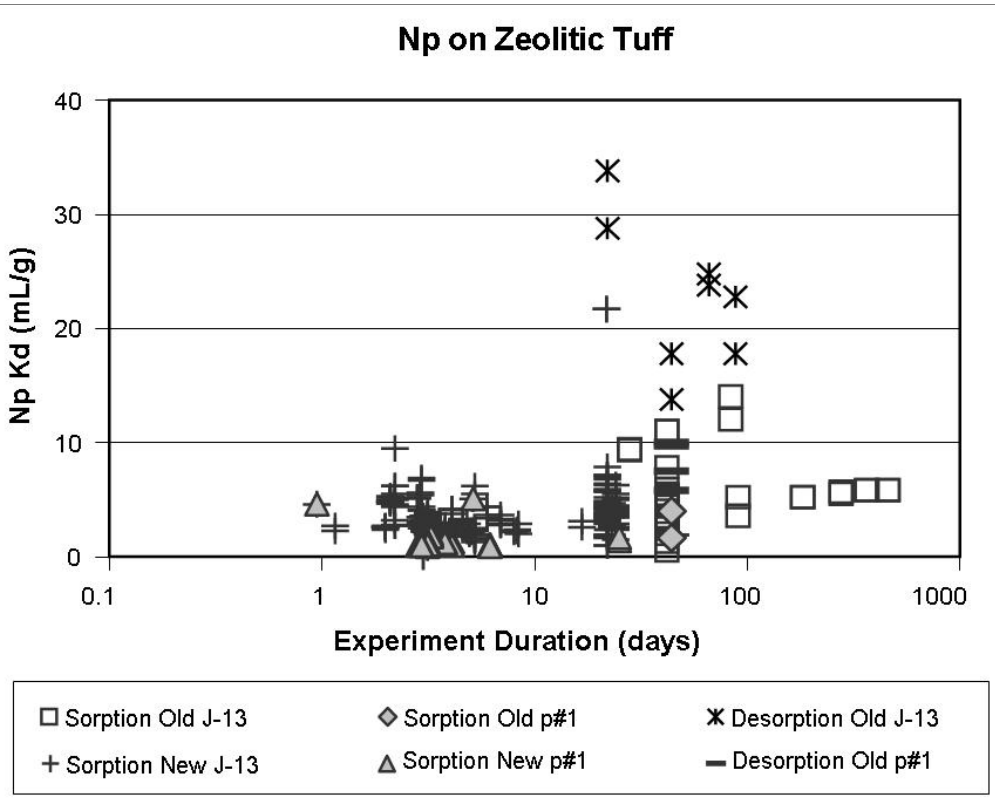

Sources: DTNs: LA0305AM831341.001 [DIRS 163789]; LA0407AM831341.004 [DIRS 170622].

NOTE: In the legend, 'old' stands for data collected before Ma y 1989, 'new' stands for data collected after May 1989. Oversaturated experiments have been omitted.

Figure A-19. Neptunium Sorption Coefficients on Zeolitic Tuff versus Experiment Duration for Sorption (Forward) and Desorption (Backward) Experiments

The impact of variations in pH on neptunium coefficients for sorption on zeolitic tuffs is shown in Figure A-20. There is a lot of scatter in the "new" data, and there do not appear to be clear positive or negative trends among these data points. It is interesting that zeolitic tuffs show a similar range of sorption coefficients as do devitrified tuffs in spite of the fact that zeolitic tuffs have approximately 10 times the surface area of devitrified tuffs. This suggests that neptunium cannot access the internal surface areas of the zeolites in the zeolitic tuffs. The neptunium sorption-coefficient probability distribution selected for zeolitic tuff in the saturated zone is a truncated normal distribution with a range of 0 to 6 mL/g, a mean of 2.88 mL/g, and a standard deviation of 1.47 mL/g. The low end of the chosen range is selected based on the minimum value obtained in short-term experiments (up to 21 days). The upper end of the distribution was chosen as a minimum upper limit with a neptunium concentration near the solubility limit (Figure A-18). It is acknowledged that a higher limit could be selected for the upper end of the distribution based on the available data.

The analysis presented in this appendix supports the model component of the saturated zone (SZ) transport model that deals with colloid-facilitated transport of radionuclides that are attached reversibly to the colloids, and in particular the adoption of the advection–dispersion equation to model colloid transport (Section 6.4.2.6). The results of this analysis do not form a direct input to the site-scale SZ transport model.

The radioisotopes of plutonium and americium can sorb either reversibly or irreversibly onto colloids with the relative percentages of these obtained from an analysis of waste form degradation and waste package corrosion processes occurring in the repository near-field environment as shown in *Saturated Zone Colloid Transport* (BSC 2004 [DIRS 170006], Section 6.3.). In general, the majority of the plutonium and americium sorbed onto colloids is irreversibly sorbed, with a typical percentage being 90% to 99% irreversible and 1% to 10% reversible as shown in *Waste Form and In-Drift Colloids-Associated Radionuclide Concentrations: Abstraction and Summary* (SNL 2007 [DIRS 177423], Section 6.3.12.2). Radionuclides that are irreversibly sorbed are typically embedded in the colloid or are so strongly sorbed onto the colloid that there is no possibility of detachment for typical transport time scales (thousands of years) through the saturated zone. On the other hand, reversibly sorbed colloids have measurable desorption rates. The irreversibly sorbed radionuclides are taken to transport in a manner identical to the colloids onto which they are sorbed. The colloid retardation factor distributions for irreversible colloids are developed in *Saturated Zone Colloid Transport* (BSC 2004 [DIRS 170006]), so only a brief description is provided here. The transport of the colloids is simulated using the advection–dispersion equation, and colloids are taken to not diffuse. Several field observations have suggested that a small percentage of colloids transport with essentially no retardation in groundwater (Kersting et al. 1999 [DIRS 103282], pp. 56 and 58; Penrose et al. 1990 [DIRS 100811], p. 228), whereas the majority undergoes either reversible or irreversible filtration, which can be described by a retardation factor, R_{col}. In this analysis, filtration is defined as the net effect of chemical sorption of the colloid onto the rock surface and the physical removal of colloids from the advective flow due to sieving and settling. The value of R_{col} is dependent on several factors such as colloid size, colloid type, and geochemical conditions (e.g., pH, Eh, and ionic strength). These factors are folded into the distribution of R_{col} that has been developed from field and experimental data collected under varying geochemical conditions with different colloid types and sizes as shown in *Saturated Zone Colloid Transport* (BSC 2004 [DIRS 170006] Section 6.4.2). Attachment rate constants, k_{att}, detachment rate constants, k_{det}, of colloids to the rock matrix and R_{col} distributions are related by:

$$R_{col} = 1 + \frac{k_{att}}{k_{det}} \qquad \text{(Eq. B-1)}$$

The attachment rate constant is also used to determine the fraction of the colloids that transport with no retardation. Specifically, colloids for which one over the attachment rate constant is smaller than the travel time through the system will transport with no retardation. The development of R_{col} distributions for the volcanics and the alluvium as well as the fraction of colloids that transport unretarded is documented in *Saturated Zone Colloid Transport* (BSC 2004 [DIRS 170006]).

The saturated zone transport simulations of radionuclides that are reversibly attached to colloids are conducted for radioisotopes of plutonium, americium, thorium, protactinium, and cesium (the rationale for selection of these radionuclides is given in *Waste Form and In-Drift Colloids-Associated Radionuclide Concentrations: Abstraction and Summary* (SNL 2007 [DIRS 177423], Section 6.3). Plutonium and americium inventories are split into reversibly and irreversibly sorbed fractions. For the reversibly sorbed transport simulations, radioisotopes of plutonium are transported as one group, radioisotopes of plutonium, thorium, and protactinium are transported as a second group, and cesium is transported as a third group. Americium, thorium, and protactinium are being treated as a single group based on the similarity in their absorption characteristics–each of these three radionuclides are strongly sorbed to surfaces generally involving the hydroxide group, and each of them displays a single valance state in solution and sorption (Allard et al. 1983 [DIRS 162982], pp. 9, 10, and 12). The radionuclides that are reversibly absorbed onto colloids are modeled using the K_c model, which represents the equilibrium partitioning of radionuclides between the aqueous phase and the colloidal phase with the distribution coefficient K_c (Robinson et al. 1997 [DIRS 100416], Equation 8-10, p. 8-35). The K_c model is a simplified colloid transport model that applies under the following conditions:

1. Contaminants sorb reversibly to the colloids in addition to interacting with the rock matrix and fractures

2. Colloids are isolated to the fracture and possess dispersive properties equivalent to that of an aqueous solute

3. Colloids interact reversibly with the rock surface

4. Colloids exist throughout the flow system.

Under these conditions, a transport equation for a contaminant attached to colloids can be written as:

$$R_{\text{col}} \frac{\partial C_c}{\partial t} = D_z \frac{\partial^2 C_c}{\partial z^2} - v \frac{\partial C_c}{\partial z} \qquad \text{(Eq. B-2)}$$

where

C_c = concentration of contaminants attached to colloids
R_{col} = a retardation factor that captures the details of colloid attachment/detachment and reversible filtration processes
v = porewater velocity
t = time
z = spatial coordinate
D_z = coefficient of longitudinal dispersion.

Equation B-2 represents a mass balance of solute sorbed to colloids, not to colloids alone.

Table C-2. Spatial Correlation Parameters for Mineralogic Rock Type Data

Direction	Range (m)	Sill
Horizontal	1,000	0.25
Vertical	75	0.35

Output DTN: LA0309RP831321.001, files: mineralogy_calculations\variogram_calculations\output\test_hor_10.var and test_ver_2.var. The values listed in this table were evaluated by visual curve fitting using interactive features of GSLIB.

Table C-3. Proportions of Zeolitic and Devitrified Rocks in Output Realizations

Realization	Zeolitic	Devitrified
1	0.6106	0.3894
2	0.5746	0.4254
3	0.6034	0.3966
4	0.5890	0.4110
5	0.6270	0.3730

Output DTN: LA0309RP831321.001, directory: \mineralogy_calculations\rocktype_distributions\output, files: rocktype.26.out, rocktype.28.out, rocktype.32.out, rocjtype.37.out, rocktype.39.out. Each file contains a list of indicator values with 1 representing zeolitic and 0 representing devitrified mineralogy. The values reported in this table are averages of the indicator values, reported in the files rocktype21-30.dbg and rocktype31-40.dbg.

Table C-4. Statistical Distributions of Experimentally Observed K_d Values

Radionuclide	Rock-type	Distribution	Mean (mL/g)	Standard Deviation (mL/g)	Minimum (mL/g)	Maximum (mL/g)
Uranium	Zeolitic	Truncated Normal	12.0	3.6	5.0	20.0
	Devitrified	Truncated Normal	2.0	0.6	0.0	4.0
Cesium	Zeolitic	Exponential	16,942.0	14,930.0	4,000.0	42,000.0
	Devitrified	Truncated Normal	728.0	464.0	100.0	1,000.0
Neptunium	Zeolitic	Truncated Normal	2.88	1.47	0.0	6.0
	Devitrified	Exponential	0.69	0.71	0.0	2.0
Plutonium	Zeolitic	Beta	100.0	15.0	50.0	300.0
	Devitrified	Beta	100.0	15.0	50.0	300.0

Source: Table A-4.

These distributions were used to derive the CDFs for each radionuclide for each rock type using software routine *calc_cdf.c* (*calc_cdf.c* V1.0, STN: 10924-1.0-00; SNL 2000 [DIRS 149117]). For each CDF, indicators were defined at four CDF cutoffs: 0.2, 0.4, 0.6, and 0.8. As mentioned earlier, in the absence of spatial data, correlation length was parameterized, and four different correlation lengths were used to generate stochastic realizations. This effect of correlation length was studied only for uranium. For other radionuclides, a correlation length of 500 m was used. Fifty different realizations were generated for each radionuclide and each rock type. Statistics of

the output realizations were calculated and compared against the input data. The software routine *calc_cdf.c* was used to calculate the CDF from the statistical realizations. Tables C-5 through C-8 compare the mean CDFs (calculated from 50 realizations) with the input CDFs for the four cutoffs.

Table C-8. Comparison of Input and Mean Output CDFs for Plutonium

Zeolitic			Devitrified		
K_d (mL/g) Cutoff	Input CDF	Output CDF	K_d (mL/g) Cutoff	Input CDF	Output CDF
87.005	0.2	0.2054	87.005	0.2	0.2018
95.094	0.4	0.4229	95.094	0.4	0.4059
102.743	0.6	0.5852	102.743	0.6	0.5976
112.348	0.8	0.7855	112.348	0.8	0.8058

Output DTN: LA0309RP831321.003.

CDF = cumulative distribution function.

C1.3.2 Results of Breakthrough Curve Calculations Using the Particle-Tracking Algorithm

These multiple K_d realizations were used to compute BTCs and model the sorption behavior of each radionuclide. A two-step approach was used. In the first step, steady-state flow fields were computed for 50 different permeability realizations. The properties used for these calculations are shown in Table C-9.

Table C-9. Values of Properties Used in Flow and Transport Calculations

Property	Value
Matrix porosity	0.22 [a]
Rock bulk density	1,997.5 kg/m^3 [a]
Flowing interval porosity	0.001 [a]
Flowing interval spacing	19.49 m [a]
Hydraulic gradient	2.9×10^{-4} [b]

Sources: [a]Value chosen to fall within the range given in Table 4-2.
[b]DTN: LA0511SK831214.001[DIRS 175769] (data qualified in BSC 2006 [DIRS 180708]).

The steady-state flow fields were used in the particle-tracking calculations. In these calculations, 4,000 particles were released along one face of the model and were allowed to move under the influence of the steady-state flow field. The locations of the particle releases were determined by a flux-weighted placement scheme. As mentioned in Section C1.1, two sets of particle-tracking calculations were performed for each steady-state flow field. In the first set of calculations, the baseline BTC was calculated for transport with diffusion from fracture to matrix and no matrix sorption. In the second set of calculations, the BTC was calculated for transport with diffusion followed by sorption on the matrix. For these calculations, the stochastically generated K_d distributions were used. The values of the diffusion coefficient used for these calculations are shown in Table C-10.

Table C-10. Values of Diffusion Coefficients Used for the Particle-Tracking Calculations

Radionuclide	Diffusion Coefficient (m^2/s)
Anion (uranium)	3.2×10^{-11}
Cation (plutonium, cesium, neptunium)	1.6×10^{-10}

Source: DTN: LA0003JC831362.001 [DIRS 149557] (Data qualified in Appendix K).

These BTCs were used to calculate the effective K_d values using the procedure described in Section C1.1. The procedure was repeated for 50 realizations of K_d. The statistics of the calculated effective K_d values are provided in Table C-11. These calculations of stochastic realizations of K_d were performed using a correlation length of 500 m. As can be seen from the results, the effective K_d distributions are very narrow compared to the distributions of experimentally observed K_d values.

Table C-11. Statistics of Calculated Effective K_d Values

Radionuclide	Distribution	Mean	Standard Deviation	Minimum	Maximum
Uranium	Truncated Normal	6.61	0.61	5.39	8.16
Cesium	Truncated Normal	5,188.72	941.55	3,000.59	6,782.92
Plutonium	Truncated Normal	110.17	7.45	89.90	129.87
Neptunium	Truncated Normal	1.48	0.23	0.99	1.83

Output DTNs: LA0309RP831341.001; LA0309RP831341.002 ; LA0309RP831341.003; LA0309RP831341.004.

A comparison was made as to how well the calculated effective K_d values predicted the particle breakthrough behavior with respect to the breakthrough behavior predicted by the heterogeneous K_d field (from which the effective value was calculated). In these calculations, a uniform value of K_d equal to the effective K_d value was used. Figure C-6 shows the two BTCs for one of the K_d realizations. The effective value of K_d calculated for this realization was 7.32 (mL/g). As can be seen from the figure, the calculated effective K_d value captures the breakthrough behavior of the heterogeneous K_d field very well.

a column experiment with material from Borehole NC-EWDP-19D. The sieving technique (wet versus dry) had only a minor effect on the mineral composition of the 75- to 500-μm fraction of the 19D sample.

Table G-1. Boreholes and Sample Preparation Methods

Borehole Location	Depth (ft BLS)	Sample Preparation Method	Particle Size Fraction (wt %)		
			75 to 2,000 μm	75 to 500 μm	< 75 μm
2D	395 to 400	A	—	59	41
2D	400 to 405	A	—	60	40
2D	405 to 410	A	—	56	44
2D	410 to 415	A	—	56	44
9S	145 to 150	A	—	66	34
9S	150 to 155	A	—	62	38
9S	155 to 160	A	—	61	39
9S	160 to 165	A	—	61	39
3S	60 to 65	A	—	54	46
3S	65 to 70	A	—	64	36
3S	70 to 75	A	—	59	41
3S	75 to 80	A	—	66	44
1X	390 to 395	B	40	39	21
1X	395 to 400	B	71	19	10
1X	400 to 405	B	33	45	22
1X	405 to 410	B	51	33	16
19D	405 to 425	A	ND	ND	ND
19D	405 to 425	C	100	0	0
19D	405 to 425	C	0	0	100

Source: Ding et al. 2003 [DIRS 164737)].

NOTES: A) Grind, crush, and dry sieve; B) Collect 75- to 2,000- μm particle materials by dry sieving without grinding or crushing, followed by process A; C) Collect 75- to 2,000-μm particle materials by dry sieving without grinding or crushing processes, follow with washing out the fine particles and collecting particle size range 75- to 2,000-μm materials by wet sieving.

BLS = below land surface; ND = not determined.

Table G-2. Borehole NC-EWDP-03S and NC-EWDP-19D Water Composition

Species	Concentration (mg/L)		
	3S (449 ft BLS)	19D1 (412 to 437 ft + 490 to 519 ft BLS)	19D2 (412 to 437 ft BLS)
Na^+	141	69.4	73.2
K^+	2.99	3.61	3.92
Li^+	0.26	0.087	0.081
Ca^{2+}	0.94 ± 0.01	7.59	7.70
Mg^{2+}	0.14	0.65	0.69
Mn^{2+}	< 0.002	0.0088	< 0.001
$Fe^{2+/3+}$	0.02	0.09	< 0.01
Al^{3+}	0.34	0.05	0.002

Table G-2. Borehole NC-EWDP-03S and NC-EWDP-19D Water Composition (Continued)

Species	Concentration (mg/L)		
	3S (449 ft BLS)	19D1 (412 to 437 ft+ 490 to 519 ft BLS)	19D2 (412 to 437 ft BLS)
SiO_2	48.4	58.0	58.4
F^-	3.24	1.78	1.96
Cl^-	8.68	5.61	6.52
NO_3^-	0.28	4.18	4.84
SO_4^{2-}	50.0	23.0	23.8
HCO_3^-	261	168	146
CO_3^{2-}	ND	0	17.9

Source: DTN: LA0705MD150304.001 [DIRS 181309].

[a] SHE is the reference electrode for reporting Eh data. $Eh(SHE)_{sample} = Eh(SHE)_{measured\ for\ sample} + [((285-2.0*(T-25))-Eh(SHE)_{measured\ for\ 7.0\ buffer}]$.

BLS=below land surface; ND=not determined; SHE=standard hydrogen electrode.

Table G-3. Mineral Abundance and Surface Areas for Selected Alluvium Samples Used in Neptunium Sorption Tests

Alluvium				Quantitative Mineral Abundance for Alluvium Samples (wt %)											Surface Area (m^2/g)	Sample Number
Sieve Method	Bore-hole	Depth (ft BLS)	PS (μm)	Smec-tite	Clino-ptilolite	Kao-linite	Mica	Tridy-mite	Cristo-balite	Quartz	Feld-spar	Calcite	Hema-tite	Total		
Dry	2D	410 to 415	75 to 500	2±1	4±1	1±1	trace	3±1	16±1	18±1	54±8	—	1±1	99±8	4.82	1
	9Sx	160 to 165	75 to 500	6±2	3±1	—	trace	1±1	18±1	14±1	58±8	—	Trace	100±8	16.49	2
	3S	75 to 80	75 to 500	1±1	13±1	1±1	1±1	—	10±1	17±1	53±8	4±1	—	100±8	11.82	3
	19D	405 to 425	75 to 500	5±2	7±1	1±1	Trace	3±1	13±1	20±2	52±8	Trace	Trace	101±9	9.45	4
	2D	410 to 415	<75	4±1	7±1	1±1	1±1	5±1	14±1	17±1	53±8	—	1±1	103±8	9.58	5
	2D	395 to 400	<75	10±3	13±1	1±1	Trace	4±1	13±1	11±1	47±7	1±1	Trace	100±8	18.34	6
	9Sx	155 to 160	<75	19±6	3±1	Trace	1±1	4±1	14±1	12±1	50±7	—	Trace	103±9	28.85	7
	3S	60 to 65	<75	7±2	13±1	2±1	1±1	1±1	11±1	12±1	44±7	9±1	Trace	100±8	26.54	8
Wet	19D	405 to 425	75 to 2,000	4±1	5±1	1±1	1±1	3±1	16±1	16±1	49±7	—	1±1	96±8	5.89	9
	19D	405 to 425	<75	48±14	6±1	1±1	1±1	2±1	5±1	8±1	29±4	1±1	—	101±15	N/A	10
	3S	65 to 70	<75	30±9	21±2	1±1	2±1	Trace	2±1	5±1	25±4	12±1	—	98±10	N/A	11

Sources: LA0401MD831322.001 [DIRS 180903], LA0401MD831322.003 [DIRS 180905], LA0412MD831341.001 [DIRS 180906].

NOTE: Surface area measurements were conducted using a NOVA 1200 High Speed Gas Sorption Analyzer.

BLS = below land surface; PS = particle size; "—" = not detected; Trace = amount at less than 0.5 wt %.

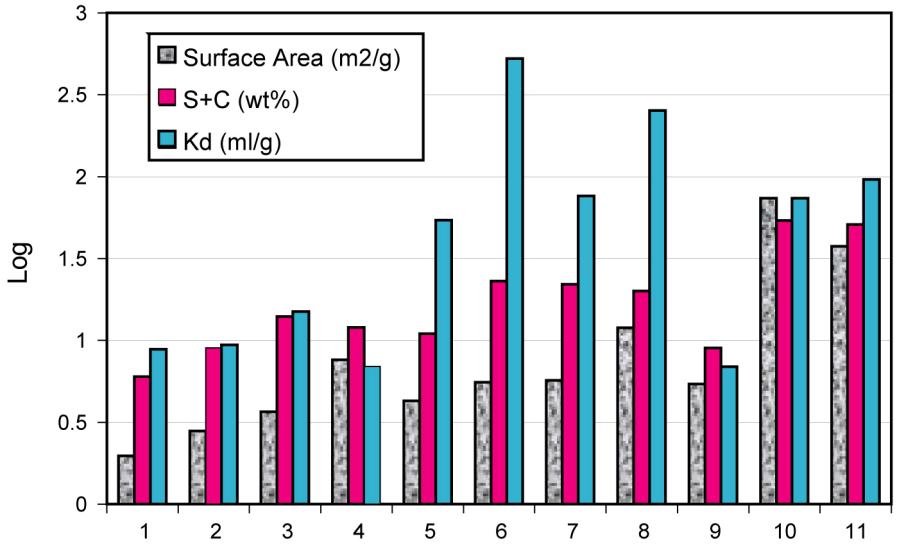

Sources: DTNs: LA0401MD831322.001 [DIRS 180903], LA0401MD831322.003 [DIRS 180905], LA0412MD831341.001 [DIRS 180906], LA0412MD831341.001 [DIRS 180906].

NOTE: Surface area units = m^2/g, S = smectite (wt %); C = clinoptilolite (wt %), K_d units = mL/g. The Y axis represents the log-values of the three variables as shown in the legend of graph. The X-axis represents the Sample Identification Numbers reported in the last column of Table G-3.

Figure G-5. Surface Area, Combined Smectite and Clinoptilolite, and K_d Values for Np(V)

G3.2 NEPTUNIUM AND URANIUM RESULTS FROM SECOND SET OF SORPTION AND DESORPTION EXPERIMENTS

The alluvium samples used in the second set of batch sorption experiments were dry sieved for most experiments. Groundwater used in the experiments was obtained from Boreholes NC-EWDP-19D (Zones 1 and 4) and NC-EWDP-10SA. The chemical composition of Borehole NC-EWDP-19D waters is summarized in Table G-5.

The mineralogy of the alluvium used in the experiments was determined by quantitative XRD (Table G-6). The major phases in the alluvium samples are silica (i.e., quartz, tridymite, cristobalite), K-feldspar, and plagioclase. The amount of smectite and clinoptilolite in the alluvium differs for the different samples. Among these samples, the sum of the smectite and clinoptilolite in Borehole NC-EWDP-22SA is larger than in NC-EWDP-19IM1A or NC-EWDP-10SA.

G.3.2.1 Batch K_d Values for ^{129}I, ^{99}Tc, ^{233}U, and ^{237}Np in Alluvium

Under ambient conditions, measured K_d values were not statistically distinguishable from zero for ^{129}I and ^{99}Tc sorption onto the alluvium, and the reproducibility of the K_d measurements was poor (Figure G-6). These results are consistent with earlier results for these two radionuclides in experiments involving alluvium and groundwater from the Phase I Nye County wells.

Table G-5. Chemical Composition of NC-EWDP-19D Waters

Species	Concentration (mg/L) in Zone 1	Concentration (mg/L) in Zone 4
pH	8.3	8.9
Na^+	79	107
K^+	3.6	3.4
Ca^{2+}	5.9	0.96
Mg^{2+}	0.56	0.035
SiO_2	59	60
F^-	1.8	2.4
Cl^-	6.3	5.8
SO_4^{2-}	23	18
HCO_3^-	190	211

Source: DTN: GS011108312322.006 [DIRS 162911].

NOTE: pH and Eh were measured in the laboratory under the conditions of the batch sorption and column transport experiments.

Table G-6. Quantitative X-ray Diffraction Results of Alluvium Used in Second Set of Experiments

	Abundance (wt%)					
	NC-EWDP-19IM1A		NC-EWDP-10SA		NC-EWDP-22SA	
Minerals	725 to 730[a, b]	785 to 790	665 to 670[b]	695 to 700	522 to 525[b]	660 to 665
Smectite	6.9[b]	6.2	5.7[b]	2.6	8.3[b]	4.7
Kaolinite	1.2	1.3	0.8	0.5	2.0	1.1
Clinoptilolite	7.7[b]	8.5	7.0[b]	4.1	14.3[b]	7.9
Tridymite	7.6	7.9	3.5	2.3	8.5	10.2
Cristobalite	5.8	6.4	7.0	5.9	5.6	7.2
Quartz	19.2	16.1	14.0	6.0	12.8	17.3
K-Feldspar	23.7	25.8	29.7	32.5	22.7	25.0
Plagioclase	25.0	26.5	30.5	40.7	19.1	21.2
Biotite	1.0	3.0	3.1	2.5	2.4	2.1
Hematite	0.7	0.7	0.8	2.4	1.0	2.5
Total	98.8	102.3	102.3	99.6	96.7	99.2

Source: DTN: LA0401MD831322.002 [DIRS 180904].

[a] Interval below land surface (feet).
[b] Samples selected to conduct kinetic adsorption of ^{233}U.

NOTE: Samples were dry sieved to retain particle sizes 75 to 500 μm.

G4. COLUMN TRANSPORT EXPERIMENTS

G4.1 NEPTUNIUM COLUMN TRANSPORT EXPERIMENTS

Two sets of column experiments were performed to investigate Np(V) transport behavior in saturated alluvium under flowing conditions. Tables G-7 and G-8 list individually the columns used and conditions in the two studies. In all the column experiments, tritium (^{3}HHO) was used as a nonsorbing tracer. Water from NC-EWDP-03S was used in the experiments in columns 1 and 2, and water from NC-EWDP-19D was used in the experiments in columns 3, 4, and 5. The alluvium used to pack the columns was wet sieved in all cases to remove fine particles that would clog the columns. The latter set of experiments was reported by Ding et al. (2003 [DIRS 164737]).

Table G-7. Np(V) Column Study (I)

	Columns 1 and 2
Geologic Medium	Alluvium in Well NWDP-03S
Interval (ft. BLS)	65 to 70
Particle Size (μm)	75 to 500
Water Used	−03S
Diameter, cm	1.0
Length of column (cm)	60
Flow rate (mL/h)	2 (reduced to 0.5 mL/h late in the test)

Source: DTN: LA0409MD831341.004 [DIRS 180925], LA0409MD831341.005 [DIRS 180926].
BLS=below land surface.

Table G-8. Np(V) Column Study (II)

	Column 3	**Column 4**	**Column 5**
Geologic Medium	Alluvium in Well NWDP-19D	Alluvium in Well NWDP-19D	Alluvium in Well NWDP-19D
Interval (ft. BLS)	405 to 425	405 to 425	405 to 425
Particle Size (μm)	75 to 2,000	75 to 2,000	75 to 2,000
Water Used	19D	19D	19D
Diameter, cm	2.5	2.5	2.5
Length of column (cm)	45	45	45
Porosity in column	0.38	0.37	0.34
Flow rate (mL/h)	10, 0.6 (2 tests)	3	10

Source: DTNs: LA0408MD831341.007 [DIRS 180927], LA0409MD831341.001 [DIRS 180928], LA0409MD831341.002 [DIRS 180929], LA0409MD831341.003 [DIRS 180930].

NOTE : columns labeled 3 and 4 in this table are labeled 1 and 2 in the source DTNs.

BLS = below land surface.

Figure G-12 shows the breakthrough curves (BTCs) of neptunium from columns 1 and 2, and Figure G-13 shows the BTCs of neptunium from columns 3, 4, and 5. The reproducibility of the two identical experiments in columns 1 and 2 (Figure G-12) is quite good, particularly with

The observed differences in neptunium transport as a function of flow rate cannot be explained by a single rate-limited sorption reaction. It is likely that multiple reactions with multiple rates were occurring in the columns because of multiple sorption sites. An approach to modeling these experimental results is discussed later in this appendix. The column experiments reveal that reactive transport processes in heterogeneous alluvium, even at a relatively small scale, are quite complicated and not amenable to simple transport models, at least when flow velocities are high.

G4.2 URANIUM COLUMN TRANSPORT EXPERIMENTS

Continuous-flow column experiments involving ^{233}U were conducted at room temperature and under ambient conditions at an initial elution rate of 10 mL/hr. The elution rate was decreased first to 5 mL/hr and then very quickly to 3 mL/hr as the experiments progressed (DTN: LA0401MD831361.001 [DIRS 166696]). Experimental conditions are presented in Table G-9. The ^{233}U BTCs relative to ^{3}HHO are shown in Figure G-14. In all cases, a small fraction of the uranium broke through at almost the same time as the ^{3}HHO, but the vast majority of the uranium mass was significantly retarded. Total uranium recoveries ranged from 26% to 65% of the uranium injected. The long tails and incomplete recoveries observed in the column experiments indicate that some of the ^{233}U was slow to desorb from the columns within the time frame of the experiments. These experiments have not yet been quantitatively interpreted to obtain estimates of uranium sorption parameters, but the modeling approach discussed later in this appendix is capable of qualitatively explaining the observed behavior.

Table G-9. Uranium Column Experiments

	Column #1	**Column #2**	**Column #3**
Geological Medium	19IM1A	10SA	22SA
Interval (ft. BLS)	725 to 730	665 to 670	522 to 525
Particle Size (μm)	75 to 2,000	75 to 2,000	75 to 2,000
	Column #1	**Column #2**	**Column #3**
Water Used	19D Zone 1	10S	19D Zone 1
Diameter, cm	2.5	2.5	2.5
Dry alluvium packed in column (g)	374.61	356.59	390.72
Water weight after the saturation (g)	89.82	102.4	85.98
Pore volume at which flow rate change to 5 ml/hr	2.2	1.8	2.3
Pore volume at which flow rate change to 3 ml/hr	2.7	2.3	2.9

Source: DTN: LA0401MD831361.001 [DIRS 166696].

NOTE: The length of columns 1, 2, and 3 are 45, 47, and 45 (cm), respectively. The flow rate for all three columns is 10 mL/h.

BLS=below land surface.

I1.3 DESCRIPTION OF THE DATA TO BE QUALIFIED

The data that were evaluated and documented in this qualification report are published in *Groundwater Chemistry Along Flow Paths Between a Proposed Repository Site and the Accessible Environment* (Ogard and Kerrisk 1984 [DIRS 100783]). These data are shown in Table I-1.

Table I-1. Compositions of Waters from UE-25 J-13 and UE-25 p#1

Chemical Constituent	UE-25 J-13 Well Water	UE-25 p#1 (Carbonate) Water (mg/L)
Ca^{2+}	11.5	87.8
Mg^{2+}	1.76	31.9
Na^{+}	45	171
K^{+}	5 .3	13.4
SiO_2	64.2	37.3[a]
Cl^{-}	6.4	37
F^{-}	2.1	3.5
SO_4^{2-}	18.1	129
HCO_3^{-}	143	698
pH	6.9	6.7

Source: Ogard and Kerrisk 1984 [DIRS 100783] data.

[a] Value derived from Table III of Ogard and Kerrisk 1984 [DIRS 100783], equivalent to 0.62 mmol/L Si.

I2. QUALIFICATION METHOD AND EVALUATION CRITERIA

The method used to qualify the data in this report is corroborating data (SCI-PRO-001, Attachment 3, Method 2). The confidence in the data is in question because data collection procedures are unavailable for review.

A comparison of the unqualified data and available qualified corroborating data will be conducted to determine that the unqualified data is acceptable and confidence in the data is established.

The following data qualification attributes will be used:

1. Extent and quality of corroborating data
2. Agreement between the data being qualified and the corroborating data
3. The importance of the data to showing that the proposed U.S. Department of Energy repository design meets the performance objectives of 10 CFR 63 [DIRS 180319].

I3. EVALUATION RESULTS

The compositions reported by Ogard and Kerrisk (1984 [DIRS 100783]) for J-13 well and p#1 waters were used in the analysis presented in Appendix A because many of the sorption coefficient experiments used in this analysis were performed in the early 1980s. Thus, to make

the comparisons of experimental data and model results more direct, the Ogard and Kerrisk (1984 [DIRS 100783]) data were used in the analysis. The Ogard and Kerrisk (1984

SCI-PRO-001. As noted in *Saturated Zone Site-Scale Flow Model* (SNL 2007 [DIRS 177391], Section A7.3.1), the uncertainty in concentration of major anions and cations is on the order of 10% for most species and 15% for F^-. Thus the data from the two sets can be expected to agree within 20% of each other. As shown in Column 4 of the Table I-3, this holds for all the constituents except Cl^-. The Ogard and Kerrisk (1984 [DIRS 100783]) value for Cl^- is somewhat higher than this range. However, because the data are used for setting limits on the range of compositional values, this is considered acceptable. Thus, the Ogard and Kerrisk (1984 [DIRS 100783]) data for the composition of the water sample from UE-25 p#1(carbonate) meet the qualification requirements.

Table I-3. Comparison of Compositions of Water from UE-25 p#1(Carbonate)

Chemical Constituent	Corroborating Data (mg/L) [a]	Concentration (mg/L) [b]	% Difference Absolute Value(100*(Column2 − Column3)/Column2)
Ca^{2+}	100	87.8	12
Mg^{2+}	39	31.9	18
Na^+	150	171	14
K^+	12	13.4	12
SiO_2	41	37.3[c]	9
Cl^-	28	37	32
F^-	N/D	3.5	N/A
SO_4^{2-}	160	129	19
HCO_3^-	694	698	0.5
pH	6.6	6.7	N/A

Sources: [a] Corroborating Data DTN: MO0007MAJIONPH.011 [DIRS 151524].
[b] Ogard and Kerrisk 1984 [DIRS 100783] data.
[c] Value derived from Table III of Ogard and Kerrisk 1984 [DIRS 100783], equivalent to 0.62 mmol/L Si.

I4. RESULTS

The qualification team determined, based on the discussions above, that the referenced data are both reasonable and appropriate for the application. This evaluation did not produce any new data.

I5. CONCLUSION

The data qualification effort documented in this report was performed in accordance with the requirements of the approved data qualification plan included in this appendix. The approved qualification method, corroborating data, was implemented as required. As a result of this qualification evaluation, these data are qualified for inclusion in this report.

Table J-1. Quantitative X-ray Diffraction Results for Alluvium Used in Long-term Uranium and Neptunium Desorption Experiments

Mineral Phase	Well NC-EWDP-19IM1A (wt %)	Well NC-EWDP-22SA (wt %)	Well NC-EWDP-10SA (wt %)
Quartz	15.3	10.1	8.7
Plagioclase	23.0	28.4	26.0
K-Feldspar	24.4	17.5	30.6
Clinoptilolite	7.6	12.0	11.6
Mica	1.3	1.0	1.8
Kaolinite	0.5	0.2	0.4
Cristobalite	5.8	5.9	8.1
Tridymite	4.1	4.3	1.6
Opal-CT	13.6	—	—
Hematite	0.4	0.6	0.5
Smectite	4.6	19.4	8.0
Total	100.6	99.4	97.4

Source: DTN: LA0705CS150304.001 [DIRS 181762].

Table J-2. Major Ion Chemistry of Groundwaters Used in Long-term Uranium and Neptunium Desorption Experiments

Species	Concentration (mg/L) in NC-EWDP-19D Zone 1 (411' to 431' BLS) [a,d]	Concentration (mg/L) in NC-EWDP-19D Zone 4 (720' to 795' BLS) [a,e]	Concentration (mg/L) in NC-EWDP-10SA (662' to 700' BLS) [b]
Temperature (°C)	32	31	29.7
pH	8.6	8.85	7.8
Na^+	91.50	107.30	40.6
K^+	3.70	3.40	6.12
Ca^{2+}	3.70	0.92	13.8
Mg^{2+}	0.31	0.03	2.45
SiO_2	58.	59.7	55.3
F^-	2.0	2.7	2.0
Cl^-	6.10	5.60	7.0
SO_4^{2-}	22.0	18.7	19.6
HCO_3^-	189	212	129
CO_3^{2-}	12.5	21.5	0
Ionic Strength (M)[c]	0.0048	0.0054	0.0035

Sources: DTNs: [a]GS011108312322.006 [DIRS 162911]; [b]GS040108312322.001 [DIRS 179422].

NOTES: [c] Calculated from major ion chemistry.
[d] Averages of rows 18 and 19 from the source DTN for Zone 1.
[e] Averages of rows 29, 30, and 31 from the source DTN for zone 4.

BLS = Below Land Surface.

Table K-2. Range of Values of Diffusion Coefficients Used for Corroboration

	Diffusion Coefficient (m^2/s)
Lower Limit	5×10^{-12}
Upper Limit	5×10^{-10}

Source: DTN: SN0310T0502103.009 [DIRS 168763].

The values of diffusion coefficients given in Table K-1 are within the range prescribed for comparison.

K6. CONCLUSION

The qualification team determined, based on the discussions above, that the referenced data are both reasonable and appropriate for the application. This evaluation did not produce any new data. The data qualification effort documented in this report was performed in accordance with the requirements of the approved Data Qualification Plan included in this appendix. The approved qualification method, corroborating data, was implemented as required. As a result of this qualification evaluation, these data are qualified for use in the report.